Original Research Article

SAGE Open Medicine

Integrated bioinformatics analysis reveals novel key biomarkers in diabetic nephropathy

SAGE Open Medicine
Volume 10: 1–32

DOI: 10.1177/20503121221137005
journals.sagepub.com/home/smo
SAGE

Harish Joshi[1], Basavaraj Vastrad[2], Nidhi Joshi[3] and Chanabasayya Vastrad[4]

Abstract

Objectives: The underlying molecular mechanisms of diabetic nephropathy have yet not been investigated clearly. In this investigation, we aimed to identify key genes involved in the pathogenesis and prognosis of diabetic nephropathy.

Methods: We downloaded next-generation sequencing data set GSE142025 from Gene Expression Omnibus database having 28 diabetic nephropathy samples and nine normal control samples. The differentially expressed genes between diabetic nephropathy and normal control samples were analyzed. Biological function analysis of the differentially expressed genes was enriched by Gene Ontology and REACTOME pathways. Then, we established the protein–protein interaction network, modules, miRNA-differentially expressed gene regulatory network and transcription factor-differentially expressed gene regulatory network. Hub genes were validated by using receiver operating characteristic curve analysis.

Results: A total of 549 differentially expressed genes were detected including 275 upregulated and 274 downregulated genes. The biological process analysis of functional enrichment showed that these differentially expressed genes were mainly enriched in cell activation, integral component of plasma membrane, lipid binding, and biological oxidations. Analyzing the protein–protein interaction network, miRNA-differentially expressed gene regulatory network and transcription factor-differentially expressed gene regulatory network, we screened hub genes MDFI, LCK, BTK, IRF4, PRKCB, EGR1, JUN, FOS, ALB, and NR4A1 by the Cytoscape software. The receiver operating characteristic curve analysis confirmed that hub genes were of diagnostic value.

Conclusions: Taken above, using integrated bioinformatics analysis, we have identified key genes and pathways in diabetic nephropathy, which could improve our understanding of the cause and underlying molecular events, and these key genes and pathways might be therapeutic targets for diabetic nephropathy.

Keywords

Bioinformatics analysis, protein–protein interaction network, differentially expressed genes, diabetic nephropathy, novel biomarkers

Date received: 24 December 2021; accepted: 18 October 2022

Introduction

Diabetic nephropathy (DN) is a common and devastating microvascular complication of the kidneys induced by diabetes mellitus.[1] The incidence of DN is reported to be 30%–40% of patients with diabetes[2] and is the main cause of end-stage renal disease throughout the world in both developed and developing countries.[3] Numerous risk factors may affect DN progression[4]; however, how these factors affect the development of DN requires further study and no effective method has been developed. Despite important developments toward an understanding of the pathophysiology of DN, early diagnosis, therapeutic interference, and underlying molecular pathogenesis are necessary.[5] Therefore, enlightening the rare nature belonging to DN is predominant in expanding therapies to improve patient outcomes.

DN remains end-stage renal disease worldwide because of its complicated molecular mechanisms and cellular

[1]Endocrine and Diabetes Care Center, Hubbali, India
[2]Department of Pharmaceutical Chemistry, KLE Society's College of Pharmacy, Gadag, India
[3]Dr. D. Y. Patil Medical College, Kolhapur, India
[4]Biostatistics and Bioinformatics, Chanabasava Nilaya, Dharwad, India

Corresponding author:
Chanabasayya Vastrad, Biostatistics and Bioinformatics, Chanabasava Nilaya, Bharthinagar, Dharwad 580001, India.
Email: channu.vastrad@gmail.com

heterogeneity, and its prevalence raises every year.[6] Therefore, recognition of DN might offer clinicians novel tools that can be used to treat the disease. Extensive genomic investigations showing the effects of genes have accepted noticeable attention. Many key genes must be identified to develop the clinical outcome for DN patients. However, the number of biomarkers that can be used to show therapeutic effects is still limited, and prognostic factors are essential for the treatment of DN patients. Therefore, it is necessary to elucidate the detailed molecular mechanisms that are independently associated with DN.

The exact mechanisms of DN are still unknown. A number of investigations have reported possible roles of some genes and pathways such as UCP1-3[7] and JAK/STAT3 signaling pathways[8] in the development of DN. However, these reports only concentrated on any certain molecule, gene, or pathway, ignoring that the development process involves aberrant expression of a variety of genes and pathways, among which some proteins might interact with other proteins and thus play an essential role in the DN.[9] Hub genes might act as prognostic or diagnostic biomarkers or treatment targets for DN.[10–12] Therefore, it is urgent to search new biomarkers for DN with powerful genome-wide technology.

High-throughput platform next-generation sequencing (NGS) data are increasingly valued for the analysis of gene expression in DN.[13] A high-quality NGS data could potentially link molecular biomarkers to the development, diagnosis, and treatment of DN.

In the present investigation, the NGS data set (GSE142025)[14] was selected from the Gene Expression Omnibus database (GEO) (http://www.ncbi.nlm.nih.gov/geo)[15] and to identify the genes correlated to DN progression and prognosis. Using the online tool limma, differentially expressed genes (DEGs) between DN and normal control were obtained. Gene Ontology (GO) annotation and REACTOME pathway enrichment analyses were conducted to further provide an overview of the function of the screened DEGs. A protein–protein interaction (PPI) network, module, miRNA-DEG regulatory network, and transcription factor (TF)-DEG regulatory network were constructed to determine the hub genes, miRNA, and TF associated with DN. Receiver operating characteristic (ROC) curve analysis of the hub genes was carried out using pROC. The aim of this investigation was to identify key genes and pathways and to explore potential candidate biomarkers for the diagnosis and therapeutic targets in DN.

Materials and methods

Data source

The DN NGS data set GSE142025[14] was downloaded from the NCBI GEO database. The data set GSE142025 was based on the GPL20301 platform (Illumina HiSeq 4000 (Homo sapiens)), including 28 DN samples and nine normal control samples. NGS data GSE142025 have generated massive genomic data, which facilitated understanding the molecular mechanisms involved in the DN.

Identification of DEGs

Identifying a gene that is differentially expressed across experimental conditions was used to identify DEGs in the GSE142025 data set with the limma package of R language. Adjusted *p*-value was retrieved by implementing the Benjamini–Hochberg false discovery rate (FDR) correction on the original *p*-value, and a fold change threshold was preferred based on our plan to target statistically significant DEGs.[16] Only genes with a fold change > 1.35 for upregulated genes and fold change < -1.24 for downregulated genes, and adjusted *p*-value < 0.05 were considered statistically significant DEGs. A volcano plot and heat map of the identified DEGs were also constructed, using an R package.

GO and pathway enrichment analysis of DEGs

In the current investigation, the significant enrichment analysis of DEGs was assessed based on the GO and REACTOME using the ToppGene (ToppFun) (https://toppgene.cchmc.org/enrichment.jsp),[17] an online tool for functional annotation analysis. GO analysis (http://geneontology.org/)[18] is an accepted, effective method for annotating genes and gene products and for identifying unique biological aspects of high-throughput genome or transcriptome data, including three categories: biological process (BP), cellular component (CC), and molecular function (MF). REACTOME database (https://reactome.org/)[19] is a well-known pathway database for precise analysis of gene functions in biological signaling pathways, which links genomic information with higher-order functional information. To analyze the function of the identified DEGs, biologic analyses were performed using GO enrichment and REACTOME enrichment pathway analysis via ToppGene online database. $p < 0.05$ as the cutoff criterion considered statistically significant.

Construction of PPI network

The online database InnateDB interactome (https://www.innatedb.com/)[20] was used to construct the PPI network and module analysis. Cytoscape (version 3.8.1) (www.cytoscape.org/)[21] was used to visualize the PPI network of DEGs. Next, the Network Analyzer plug-in for Cytoscape was applied to calculate node degree,[22] betweenness centrality,[23] stress centrality,[24] and closeness centrality.[25] The plug-in PEWCC1[26] of Cytoscape was applied to detect densely connected regions in PPI networks. The PPI networks were constructed using Cytoscape, and the most significant module in the PPI networks was selected using PEWCC1.

Integrated regulatory network construction

The integrated regulatory network of miRNAs (microRNAs) and TFs was constructed based on the standardized integration of numerous high-throughput data sets. It granted a plan including a set of hub genes, miRNAs, and TFs for analyzing multilevel regulation in DN. The miRNAs associated with DEGs were selected from miRNet (https://www.mirnet.ca/)[27] Database (The integration database of TarBase, miRTarBase, miRecords, miRanda (S mansoni only), miR2Disease, HMDD, PhenomiR, SM2miR, PharmacomiR, EpimiR, starBase, TransmiR, ADmiRE, and TAM 2.0), and TFs associated with DEGs were selected from NetworkAnalyst database (https://www.networkanalyst.ca/)[28] Database (The integration database of JASPAR). The miRNA-DEG regulatory network and TF-DEG regulatory network were constructed by using Cytoscape software,[21] which is open-source software for visualizing complex networks.

ROC curve analysis of the hub genes

The diagnostic value of validated hub genes was assessed using ROC curve analysis using the pROC in R with GLM prediction model.[29] An area under the curve (AUC) value was determined and used to nominate the ROC effect.

Results

Identification of DEGs

DN and normal control samples (28 and 9, respectively) were first analyzed. Limma was used to identify the DEGs. Following analysis of the NGS data set GSE142025, 549 DEGs (275 upregulated and 274 downregulated) genes were identified and are listed in Table 1. The volcano plot and heat map are shown in Figures 1 and 2, respectively.

Gene ontology and pathway enrichment analysis of DEGs

The identified DEGs were uploaded to the online software ToppGene for GO and REACTOME pathway enrichment analyses and results are listed in Tables 2 and 3. The results of the GO analysis revealed that upregulated genes were significantly enriched in BP, including cell activation and regulation of the immune system process, whereas downregulated genes were significantly enriched in response to hormone and ion transport. In terms of CC, the upregulated genes were enriched in the cell surface and intrinsic component of the plasma membrane, whereas downregulated genes were enriched in the integral component of plasma membrane and nuclear chromatin. In terms of MF, the upregulated genes were enriched in signaling receptor binding and identical protein binding, whereas downregulated genes were enriched in lipid binding and transporter activity. REACTOME pathway analysis revealed that the upregulated genes were highly associated with pathways including immunoregulatory interactions between lymphoid and nonlymphoid cells and the innate immune system, whereas downregulated genes were significantly enriched in biological oxidations and GPCR ligand binding.

Construction of PPI network

The DEG expression profiles in DN were constructed according to the information in the InnateDB interactome database. The PPI network of DEGs consisted of 2718 nodes and 4477 edges (Figure 3). There are 10 genes selected as hub genes, such as MDFI, LCK, Bruton tyrosine kinase (BTK), IRF4, PRKCB, EGR1, JUN, FOS, ALB, and NR4A1 are listed in Table 4. Two significant modules were obtained from the PPI network of DEGs using PEWCC1, including 15 nodes and 36 edges (Figure 4(a)) and 7 nodes and 12 edges (Figure 4(b)). GO and pathway enrichment analysis revealed that genes in these modules were mainly involved in the innate immune system, immunoregulatory interactions between lymphoid and nonlymphoid cells, cell activation, regulation of immune system process, cell surface, response to the hormone, cytokine signaling in the immune system, metabolism of proteins, and nuclear chromatin.

Integrated regulatory network construction

The miRNA-DEG regulatory network had 8997 interactions (involving 1973 miRNAs and 248 DEGs) (Figure 5). Moreover, COL1A1 was targeted by 178 miRNAs (ex, hsa-mir-4492), IRF4 was targeted by 140 miRNAs (e.g. hsa-mir-4319), MYBL2 was targeted by 83 miRNAs (e.g. hsa-mir-637), PRKCB was targeted by 81 miRNAs (e.g. hsa-mir-1261), IL2RB was targeted by 54 miRNAs (e.g. hsa-mir-4300), JUN was targeted by 144 miRNAs (e.g. hsa-mir-3943), EGR1 was targeted by 132 miRNAs (e.g. hsa-mir-548e-3p), ZFP36 was targeted by 130 miRNAs (e.g. hsa-mir-6077), FOS was targeted by 105 miRNAs (e.g. hsa-mir-5586-5p), and DUSP1 was targeted by 97 miRNAs (e.g. hsa-mir-4458), which are listed in Table 5. The TF-DEG regulatory network had 1954 interactions (involving 81 TFs and 250 DEGs) (Figure 6). Moreover, IRF4 was targeted by 10 TFs (e.g. NFATC2), LCK was targeted by 10 TFs (e.g. YY1), RET was targeted by 10 TFs (e.g. NR2C2), MAP1LC3C was targeted by 10 TFs (e.g. MAX), IL2RB was targeted by 8 TFs (e.g. PDX1), ATF3 was targeted by 19 TFs (e.g. TP53), EGR1 was targeted by 16 TFs (e.g. ARID3A), JUNB was targeted by 15 TFs (e.g. SRF), FOS was targeted by 13 TFs (e.g. CREB1), and PTPRO was targeted by 13 TFs (e.g. NR3C1), which are listed in Table 5.

ROC curve analysis of the hub genes

Ten hub genes are prominently expressed in DN; we performed a ROC curve analysis to evaluate their sensitivity and

Table 1. The statistical metrics for key differentially expressed genes (DEGs).

Gene Symbol	logFC	*p* Value	adj. *p*. Val	t Value	Regulation	Gene Name
CFHR1	3.375351879	6.45E–06	0.000286	5.276223	Up	Complement factor H-related 1
GREM1	3.283471762	1.74E–05	0.000511	4.951466	Up	Gremlin 1, DAN family BMP antagonist
DCANP1	3.226514295	3.24E–05	0.000732	4.748378	Up	Dendritic cell-associated nuclear protein
CCL19	3.183655087	0.000478	0.003789	3.840947	Up	C-C motif chemokine ligand 19
COL6A5	3.16784535	0.000285	0.002741	4.0192	Up	Collagen type VI alpha 5 chain
LINC01426	3.062123463	4.5E–06	0.00023	5.393562	Up	Long intergenic nonprotein coding RNA 1426
PAX5	2.995750749	0.001584	0.008304	3.417456	Up	Paired box 5
IGLL5	2.912935307	0.002413	0.011125	3.263816	Up	Immunoglobulin lambda-like polypeptide 5
MROH2B	2.910264537	5.23E–07	6.86E–05	6.093034	Up	Maestro heat-like repeat family member 2B
CIDEC	2.753545271	0.012816	0.036576	2.619345	Up	Cell death-inducing DFFA-like effector c
FCRL2	2.743514071	8.69E–05	0.001309	4.420696	Up	Fc receptor-like 2
TIFAB	2.626352493	0.00019	0.002141	4.15824	Up	TIFA inhibitor
CADM3-AS1	2.618687617	1.05E–05	0.00038	5.118451	Up	CADM3 antisense RNA 1
IRF4	2.612976293	0.000493	0.003855	3.830636	Up	Interferon regulatory factor 4
SFRP2	2.607968652	2.15E–05	0.000577	4.882333	Up	Secreted frizzled-related protein 2
CCL21	2.586085816	0.000153	0.001871	4.230566	Up	C-C motif chemokine ligand 21
ABCA13	2.562866175	0.000111	0.001536	4.337509	Up	ATP-binding cassette subfamily A member 13
SCARA5	2.529702127	9.29E–06	0.000353	5.157339	Up	Scavenger receptor class A member 5
SERPINA3	2.502144721	0.000464	0.00371	3.851597	Up	Serpin family A member 3
REG1A	2.481881104	0.004645	0.017444	3.018637	Up	Regenerating family member 1 alpha
LTF	2.421786484	0.005473	0.019684	2.955879	Up	Lactotransferrin
LILRA4	2.418292874	0.001784	0.009035	3.37445	Up	Leukocyte immunoglobulin-like receptor A4
CLEC4C	2.416946253	0.005918	0.020848	2.925733	Up	C-type lectin domain family 4 member C
CNR2	2.379118466	0.000715	0.004846	3.700816	Up	Cannabinoid receptor 2
MZB1	2.375027208	0.000853	0.005455	3.638582	Up	marginal zone B and B1 cell-specific protein
ACKR1	2.37312685	0.000468	0.003733	3.848851	Up	Atypical chemokine receptor 1 (Duffy blood group)
SIRPG-AS1	2.369303021	0.000435	0.003558	3.873601	Up	SIRPG antisense RNA 1
LINC00402	2.316005734	0.003461	0.014274	3.129905	Up	Long intergenic nonprotein coding RNA 402
TUBB3	2.312688215	0.002778	0.01222	3.211856	Up	Tubulin beta 3 class III
SLPI	2.308032387	0.001018	0.006133	3.576066	Up	Secretory leukocyte peptidase inhibitor
FAM30A	2.28349722	0.003088	0.013132	3.172436	Up	Family with sequence similarity 30 member A
FCRL5	2.268813115	0.002892	0.01254	3.196939	Up	Fc receptor-like 5
MYBPC2	2.26175633	0.000555	0.004157	3.789632	Up	Myosin-binding protein C, fast type
CADM3	2.239083735	8.09E–05	0.001262	4.444443	Up	Cell adhesion molecule 3
DHRS9	2.236482299	0.000479	0.00379	3.840715	Up	Dehydrogenase/reductase 9
TMEM132D	2.208380654	0.002807	0.012294	3.207921	Up	transmembrane protein 132D
SAA1	2.204503934	0.014613	0.040281	2.565561	Up	Serum amyloid A1
SPIB	2.196829332	0.002074	0.010018	3.319507	Up	Spi-B transcription factor
VCAN	2.179158452	0.001073	0.006349	3.557221	Up	Versican
CD79A	2.177923434	0.002178	0.010386	3.301492	Up	CD79a molecule
CD5L	2.173006586	0.005788	0.020538	2.934297	Up	CD5 molecule like
CCR2	2.157792286	6.19E–05	0.001079	4.533759	Up	C-C motif chemokine receptor 2
CTSG	2.145714072	0.000928	0.005752	3.608651	Up	Cathepsin G
REG3G	2.125802371	0.009803	0.030045	2.727497	Up	Regenerating family member 3 gamma
CD1C	2.087388332	0.000239	0.002468	4.079532	Up	CD1c molecule
MEOX1	2.079477205	0.000274	0.002661	4.033198	Up	Mesenchyme homeobox 1
SIGLEC6	2.076554595	0.000292	0.002776	4.011408	Up	Sialic acid-binding Ig-like lectin 6
CD3D	2.071816063	0.000358	0.003134	3.941582	Up	CD3d molecule
CFD	2.062354119	1.08E–06	0.000104	5.856553	Up	Complement factor D
IRX6	2.061231203	9.92E–06	0.000367	5.135892	Up	Iroquoishomeobox 6
FCRLA	2.027204494	0.012459	0.0359	2.630844	Up	Fc receptor-like A
MIR4539	2.026464338	0.012999	0.036982	2.613561	Up	MicroRNA 4539
FCRL1	2.024534059	0.007425	0.024534	2.83743	Up	Fc receptor-like 1

(Continued)

Table 1. (Continued)

Gene Symbol	logFC	*p* Value	adj. *p*. Val	t Value	Regulation	Gene Name
TPSD1	2.022989682	0.003821	0.015262	3.092631	Up	Tryptase delta 1
FCER2	2.022109034	0.003407	0.014124	3.135759	Up	Fc fragment of IgE receptor II
CHI3L2	2.003241518	0.000685	0.004733	3.716022	Up	Chitinase 3-like 2
CPA4	1.99451183	0.004093	0.01598	3.066725	Up	Carboxypeptidase A4
LAX1	1.993175742	0.001055	0.006279	3.56317	Up	Lymphocyte transmembrane adaptor 1
BATF	1.973765528	0.000777	0.005137	3.671578	Up	Basic leucine zipper ATF-like transcription factor
CPA3	1.969913281	0.000963	0.00591	3.595684	Up	Carboxypeptidase A3
MS4A1	1.96899968	0.003971	0.015647	3.078143	Up	Membrane spanning 4-domains A1
IKZF3	1.966638055	0.000876	0.005547	3.629001	Up	IKAROS family zinc finger 3
MMRN1	1.96266155	0.000323	0.002939	3.976043	Up	Multimerin 1
PRRX1	1.961218687	0.000133	0.001725	4.278157	Up	Paired-related homeobox 1
STMN2	1.959795393	0.005006	0.018384	2.990093	Up	Stathmin 2
P2RX5	1.956461404	0.000661	0.004645	3.728171	Up	Purinergic receptor P2X 5
ALX1	1.956345412	9.05E–07	9.54E–05	5.914595	Up	ALX homeobox 1
ADCYAP1R1	1.95209166	0.000175	0.002033	4.185887	Up	ADCYAP receptor type I
CLEC10A	1.951812324	0.000427	0.003526	3.88015	Up	C-type lectin domain containing 10A
ANKRD36BP2	1.950150891	0.006523	0.022381	2.887996	Up	Ankyrin repeat domain 36B pseudogene 2
HAS2	1.943166549	0.000107	0.001495	4.350053	Up	Hyaluronan synthase 2
XCL2	1.943153725	0.000436	0.003558	3.873298	Up	X-C motif chemokine ligand 2
COL6A3	1.936091001	2.02E–05	0.00055	4.902623	Up	Collagen type VI alpha 3 chain
COL1A1	1.935231067	0.000407	0.003416	3.896682	Up	Collagen type I alpha 1 chain
PNOC	1.925353932	1.41E–05	0.000461	5.020732	Up	Prepronociceptin
ELK2AP	1.920474519	0.014111	0.039255	2.579944	Up	ETS transcription factor ELK2A, pseudogene
TPSAB1	1.91754716	0.001694	0.008704	3.393181	Up	Tryptase alpha/beta 1
FAP	1.911924967	0.001987	0.009744	3.335114	Up	Fibroblast activation protein alpha
FCRL3	1.903477996	0.003122	0.013244	3.168381	Up	Fc receptor-like 3
FABP4	1.899953641	0.001241	0.007	3.505186	Up	Fatty acid-binding protein 4
CD48	1.899406447	0.001164	0.006714	3.528088	Up	CD48 molecule
TPSB2	1.897530274	0.00124	0.006998	3.505525	Up	Tryptase beta 2 (gene/pseudogene)
LCK	1.89611849	0.000535	0.004065	3.802341	Up	LCK proto-oncogene, Src family tyrosine kinase
SCEL	1.894854196	0.006236	0.021667	2.905458	Up	Sciellin
ERFE	1.878168839	3.96E–05	0.000829	4.681716	Up	Erythroferrone
CD52	1.878049795	0.000603	0.004403	3.760149	Up	CD52 molecule
POU2AF1	1.871505525	0.00895	0.0281	2.76376	Up	POU class 2 homeobox associating factor 1
SIRPG	1.870479999	0.00077	0.0051	3.674724	Up	Signal regulatory protein gamma
COL3A1	1.865958016	2.87E–05	0.000683	4.788045	Up	Collagen type III alpha 1 chain
LCN2	1.862781786	0.010555	0.031821	2.697877	Up	Lipocalin 2
CD2	1.856073182	0.000754	0.005021	3.681897	Up	CD2 molecule
NTM	1.840924852	0.000389	0.003312	3.91259	Up	Neurotrimin
FUT7	1.840017016	3.41E–05	0.000755	4.731488	Up	Fucosyltransferase 7
SLAMF7	1.834242248	0.003213	0.013549	3.157672	Up	SLAM family member 7
CD1E	1.830807447	0.006558	0.022459	2.88592	Up	CD1e molecule
GZMK	1.829645137	0.000346	0.003078	3.952776	Up	Granzyme K
RHOH	1.828685222	0.002566	0.011598	3.24117	Up	Ras homolog family member H
DRP2	1.821851174	0.00618	0.021509	2.909002	Up	Dystrophin-related protein 2
MIR142	1.814768065	0.000493	0.003856	3.830368	Up	MicroRNA 142
MMP7	1.809748337	0.004486	0.01705	3.031935	Up	Matrix metallopeptidase 7
CAPN6	1.80825955	1.13E–05	0.000401	5.092733	Up	Calpain 6
SYT16	1.807911555	0.000777	0.005137	3.671545	Up	Synaptotagmin 16
MOXD1	1.804864977	6.79E–05	0.001133	4.502783	Up	Monooxygenase DBH-like 1
BLK	1.803306234	0.004077	0.015934	3.068156	Up	BLK proto-oncogene, Src family tyrosine kinase
SIT1	1.803155699	0.000496	0.003869	3.828585	Up	Signaling threshold regulating transmembrane adaptor 1
HOPX	1.796171888	0.000256	0.002565	4.056314	Up	HOP homeobox

(Continued)

Table 1. (Continued)

Gene Symbol	logFC	*p* Value	adj. *p*. Val	t Value	Regulation	Gene Name
NNMT	1.784342787	0.006993	0.023535	2.86089	Up	Nicotinamide N-methyltransferase
TRAT1	1.775053381	0.003649	0.014789	3.10998	Up	T-cell receptor-associated transmembrane adaptor 1
WFDC2	1.771619001	0.000284	0.002735	4.020844	Up	WAP four-disulfide core domain 2
ITGBL1	1.769703731	0.000175	0.002037	4.184947	Up	Integrin subunit beta-like 1
CD79B	1.759817442	0.000232	0.002421	4.08941	Up	CD79b molecule
GPR55	1.749097368	0.003456	0.014268	3.13039	Up	G protein-coupled receptor 55
TREML2	1.742142244	0.010133	0.030791	2.714259	Up	Triggering receptor expressed on myeloid cells-like 2
SYT12	1.74106022	0.000336	0.003025	3.962701	Up	Synaptotagmin 12
C3	1.717612063	0.004069	0.015917	3.068897	Up	Complement C3
CD180	1.714738347	0.00027	0.002637	4.037439	Up	CD180 molecule
JCHAIN	1.714017091	0.018656	0.048332	2.463887	Up	Joining chain of multimeric IgA and IgM
CORO1A	1.708038536	0.000546	0.004119	3.794852	Up	Coronin 1A
C16orf54	1.707976962	0.000496	0.003871	3.828267	Up	Chromosome 16 open reading frame 54
SP140	1.705740685	0.000959	0.005892	3.597091	Up	SP140 nuclear body protein
EOMES	1.69791506	0.002023	0.009872	3.32859	Up	Eomesodermin
TIMP1	1.692895338	0.000254	0.002559	4.058215	Up	TIMP metallopeptidase inhibitor 1
PIK3CD-AS1	1.6891943	0.000268	0.00262	4.041048	Up	PIK3CD antisense RNA 1
CACNA1I	1.687578495	0.017402	0.04588	2.493055	Up	Calcium voltage-gated channel subunit alpha1 I
SNX20	1.683121317	0.000882	0.005571	3.626733	Up	Sorting nexin 20
JAML	1.675564661	0.001344	0.007377	3.476748	Up	Junction adhesion molecule like
LOC100129697	1.668768968	0.000148	0.001832	4.242293	Up	Uncharacterized LOC100129697
ITPRIPL1	1.665793436	1.81E–08	7.77E–06	7.198464	Up	ITPRIP-like 1
UBASH3A	1.664469563	0.001801	0.009087	3.370952	Up	Ubiquitin-associated and SH3 domain containing A
TNC	1.64799782	0.001647	0.008518	3.403242	Up	Tenascin C
FCER1A	1.638585806	0.001944	0.009618	3.342989	Up	Fc fragment of IgE receptor Ia
SLA2	1.636314115	2.55E–06	0.000174	5.577593	Up	Src-like adaptor 2
ISLR2	1.635028281	0.000107	0.001495	4.349937	Up	Immunoglobulin superfamily containing leucine-rich repeat 2
CD244	1.632336588	0.000155	0.001889	4.226308	Up	CD244 molecule
WNT10A	1.632155168	0.000873	0.005536	3.630254	Up	Wnt family member 10A
MSC	1.628689376	0.000137	0.001757	4.268118	Up	Musculin
C1S	1.627314952	8.01E–05	0.001259	4.448022	Up	Complement C1s
APCDD1	1.62142107	5.46E–06	0.000259	5.330595	Up	APC downregulated 1
TNNI2	1.620143883	0.004636	0.017426	3.019392	Up	Troponin I2, fast skeletal type
JSRP1	1.619782863	0.018994	0.049019	2.456317	Up	Junctional sarcoplasmic reticulum protein 1
SLAMF1	1.615745199	0.001321	0.007296	3.482873	Up	Signaling lymphocytic activation molecule family member 1
ACTG2	1.609285963	0.013207	0.037402	2.607053	Up	Actin gamma 2, smooth muscle
MS4A6A	1.608244409	6.66E–05	0.00112	4.509422	Up	Membrane spanning 4-domains A6A
KCNA3	1.603063508	0.003907	0.015491	3.084266	Up	Potassium voltage-gated channel subfamily A member 3
MS4A2	1.596663199	0.004256	0.01643	3.051939	Up	Membrane spanning 4-domains A2
ITGAD	1.591699285	0.007977	0.025862	2.809286	Up	Integrin subunit alpha D
TIGIT	1.590987752	0.000204	0.002231	4.133843	Up	T-cell immunoreceptor with Ig and ITIM domains
IKZF1	1.589791641	0.001455	0.00782	3.448127	Up	IKAROS family zinc finger 1
TNFSF14	1.5884891	0.001084	0.006389	3.553428	Up	TNF superfamily member 14
LYZ	1.580296335	0.014447	0.039938	2.570264	Up	Lysozyme
GRAP2	1.576445065	0.001252	0.007046	3.502051	Up	GRB2-related adaptor protein 2
AHNAK2	1.571109664	0.000167	0.001967	4.202083	Up	AHNAK nucleoprotein 2
ZNF831	1.568415767	0.003062	0.013049	3.17558	Up	Zinc finger protein 831
IL2RB	1.566445984	0.003199	0.013512	3.159266	Up	Interleukin 2 receptor subunit beta
FCMR	1.561885784	0.006687	0.022766	2.878376	Up	Fc fragment of IgM receptor
MAP1LC3C	1.560730571	0.000833	0.005372	3.646757	Up	Microtubule-associated protein 1 light chain 3 gamma

(Continued)

Table 1. (Continued)

Gene Symbol	logFC	*p* Value	adj. *p*. Val	t Value	Regulation	Gene Name
MIR646HG	1.558223684	0.00152	0.008057	3.432328	Up	MIR646 host gene
C11orf21	1.55710188	0.002707	0.012016	3.221354	Up	Chromosome 11 open reading frame 21
GALNT5	1.555304171	0.00249	0.011382	3.252332	Up	Polypeptide N-acetylgalactosaminyltransferase 5
CRLF1	1.554989867	0.000395	0.003352	3.906861	Up	Cytokine receptor-like factor 1
TNFRSF18	1.553278623	0.014986	0.041064	2.55517	Up	TNF receptor superfamily member 18
LY9	1.552465907	0.003752	0.015073	3.099483	Up	Lymphocyte antigen 9
FAIM2	1.550957345	5.48E–05	0.001005	4.574005	Up	Fas apoptotic inhibitory molecule 2
B3GALT5	1.54952358	1.49E–05	0.000475	5.002404	Up	Beta-1,3-galactosyltransferase 5
LSP1	1.549271938	0.002195	0.010433	3.298699	Up	Lymphocyte-specific protein 1
CXCR3	1.543901965	3.29E–05	0.000736	4.743203	Up	C-X-C motif chemokine receptor 3
TMC8	1.541786417	0.002731	0.012084	3.218097	Up	Transmembrane channel-like 8
PLAC8	1.539006889	0.004196	0.016274	3.057255	Up	Placenta-associated 8
CCR5	1.534551438	0.000717	0.004852	3.69994	Up	C-C motif chemokine receptor 5 (gene/pseudogene)
CPZ	1.534329146	0.00115	0.006665	3.532378	Up	Carboxypeptidase Z
FGD2	1.534216818	0.00016	0.001923	4.216101	Up	FYVE, RhoGEF, and PH domain containing 2
GZMM	1.534073723	6.3E–05	0.001085	4.527725	Up	Granzyme M
PTCRA	1.533003325	0.01774	0.04652	2.485021	Up	Pre T-cell antigen receptor alpha
WNT7B	1.532317096	0.012504	0.035984	2.629356	Up	Wnt family member 7B
C1QA	1.529386516	0.000118	0.001603	4.317647	Up	Complement C1q A chain
NCMAP	1.52802892	0.000232	0.002421	4.089193	Up	Noncompact myelin-associated protein
CD3E	1.52793567	0.004051	0.015866	3.070568	Up	CD3e molecule
AGAP2	1.524193817	0.000524	0.004013	3.809608	Up	ArfGAP with GTPase domain, ankyrin repeat, and PH domain 2
LIMD2	1.522353012	0.000109	0.001513	4.343398	Up	LIM domain containing 2
CARD11	1.522194992	0.002737	0.012099	3.217345	Up	Caspase recruitment domain family member 11
FNDC4	1.520969705	1.9E–05	0.000533	4.924067	Up	Fibronectin type III domain containing 4
TLR10	1.514001337	0.009109	0.02846	2.756752	Up	Toll-like receptor 10
TDO2	1.512540028	0.017137	0.045409	2.499489	Up	Tryptophan 2,3-dioxygenase
THEMIS	1.509953324	0.001722	0.008804	3.387101	Up	Thymocyte selection associated
IL2RG	1.50827007	0.004489	0.017054	3.031697	Up	Interleukin 2 receptor subunit gamma
CD7	1.506857976	0.003941	0.01557	3.080958	Up	CD7 molecule
LIX1	1.50655171	0.000452	0.003651	3.860275	Up	Limb and CNS expressed 1
COL1A2	1.506450605	2.73E–05	0.000662	4.803964	Up	Collagen type I alpha 2 chain
COL14A1	1.498208524	1.53E–05	0.000483	4.994513	Up	Collagen type XIV alpha 1 chain
MDK	1.495905721	1.9E–05	0.000533	4.923384	Up	Midkine
S1PR4	1.495557063	0.000803	0.005258	3.659975	Up	Sphingosine-1-phosphate receptor 4
THBS2	1.492020577	0.002719	0.012052	3.219753	Up	Thrombospondin 2
LINC00639	1.490721153	6.3E–05	0.001085	4.528027	Up	Long intergenic nonprotein coding RNA 639
SVEP1	1.489214912	5.76E–07	7.18E–05	6.061539	Up	Sushi, von Willebrand factor type A, EGF, and pentraxin domain containing 1
ITGB6	1.484476182	0.00567	0.020218	2.94228	Up	Integrin subunit beta 6
NLRP2	1.483481562	0.013616	0.038264	2.594575	Up	NLR family pyrin domain containing 2
RAC2	1.482940025	0.00253	0.011507	3.246417	Up	Rac family small GTPase 2
GDF5	1.481858146	0.009126	0.028491	2.756031	Up	Growth differentiation factor 5
WNT7A	1.480151354	0.009367	0.028996	2.745656	Up	Wnt family member 7A
ARL11	1.478000843	0.000105	0.001482	4.355871	Up	ADP ribosylation factor-like GTPase 11
SASH3	1.475744373	0.000486	0.003823	3.835226	Up	SAM and SH3 domain containing 3
MYO1G	1.46925159	0.00231	0.010802	3.279892	Up	Myosin IG
POM121L9P	1.466153993	0.002436	0.011191	3.260415	Up	POM121 transmembranenucleoporin-like 9, pseudogene
ADH1B	1.461601913	6.74E–07	7.94E–05	6.010212	Up	Alcohol dehydrogenase 1B (class I), beta polypeptide
LAMC2	1.461355175	0.002178	0.010386	3.301482	Up	Laminin subunit gamma 2

(Continued)

Table 1. (Continued)

Gene Symbol	logFC	*p* Value	adj. *p*. Val	t Value	Regulation	Gene Name
KCNV1	1.46127346	0.013117	0.037231	2.609875	Up	Potassium voltage-gated channel modifier subfamily V member 1
PYCARD	1.46067637	1.81E–05	0.000523	4.939807	Up	PYD and CARD domain containing
PPP1R1B	1.456662604	1.38E–05	0.000453	5.027427	Up	Protein phosphatase 1 regulatory inhibitor subunit 1B
COL5A1	1.455985156	0.000318	0.002912	3.981436	Up	Collagen type V alpha 1 chain
PVT1	1.455742066	7.94E–05	0.001253	4.450892	Up	Pvt1 oncogene
DOCK2	1.454042717	0.001397	0.007597	3.462764	Up	Dedicator of cytokinesis 2
TESPA1	1.453268833	0.004016	0.015779	3.073909	Up	Thymocyte expressed, positive selection-associated 1
BTK	1.45253006	0.00131	0.007264	3.485986	Up	Bruton tyrosine kinase
C1R	1.449568949	5.04E–05	0.00096	4.602107	Up	Complement C1r
TMSB10	1.447879296	9.09E–05	0.00135	4.40552	Up	Thymosin beta 10
SH2D1A	1.4473591	0.001042	0.00624	3.567539	Up	SH2 domain containing 1A
BEND4	1.443375214	0.003126	0.01325	3.167932	Up	BEN domain containing 4
PRKCB	1.44042359	0.002978	0.012764	3.18604	Up	Protein kinase C beta
ARHGAP9	1.439086199	0.001262	0.00708	3.499239	Up	Rho GTPase-activating protein 9
CCND2	1.437614117	5.74E–05	0.001039	4.55889	Up	Cyclin D2
TBX18	1.437086398	0.000143	0.001798	4.252942	Up	T-box transcription factor 18
COMP	1.435675266	0.00041	0.003424	3.89446	Up	Cartilage oligomeric matrix protein
CP	1.435662948	0.00123	0.006951	3.508397	Up	Ceruloplasmin
ALOX5	1.433608913	0.001118	0.006542	3.542647	Up	Arachidonate 5-lipoxygenase
CD8A	1.425850241	0.001209	0.006866	3.514582	Up	CD8a molecule
CD19	1.422740485	0.012688	0.036351	2.623421	Up	CD19 molecule
CARMIL2	1.421192212	0.003508	0.014403	3.124753	Up	Capping protein regulator and myosin 1 linker 2
CD247	1.420138262	0.001154	0.006678	3.531292	Up	CD247 molecule
KCNS1	1.418903267	0.000132	0.001717	4.280475	Up	Potassium voltage-gated channel modifier subfamily S member 1
ITGAL	1.418756962	0.001832	0.009195	3.364758	Up	Integrin subunit alpha L
MIR27B	1.41850226	1.48E–10	3.63E–07	8.847112	Up	microRNA 27b
CD3G	1.412247206	0.004048	0.015859	3.070908	Up	CD3g molecule
TMSB4X	1.410654763	3.64E–05	0.000789	4.709219	Up	Thymosin beta 4 X-linked
PLCB2	1.410297586	0.000636	0.00453	3.741726	Up	Phospholipase C beta 2
ADRA2A	1.408389124	0.000621	0.004452	3.750233	Up	Adrenoceptor alpha 2A
PIK3R6	1.406728067	0.003049	0.013008	3.177219	Up	Phosphoinositide-3-kinase regulatory subunit 6
ARHGAP40	1.404436104	0.004347	0.016679	3.043845	Up	Rho GTPase activating protein 40
GZMA	1.403790925	0.000877	0.005549	3.628612	Up	Granzyme A
JAKMIP1	1.402135988	0.001308	0.007258	3.486483	Up	Janus kinase and microtubule interacting protein 1
CD200R1	1.400155752	0.000876	0.005545	3.629259	Up	CD200 receptor 1
CD84	1.400119591	0.001584	0.008304	3.417471	Up	CD84 molecule
MDFI	1.397479754	1.17E–05	0.000406	5.08128	Up	MyoD family inhibitor
RARRES1	1.396688013	0.000584	0.004307	3.771864	Up	Retinoic acid receptor responder 1
IFNG-AS1	1.394713347	0.018488	0.048011	2.4677	Up	IFNG antisense RNA 1
NCKAP1L	1.393598999	0.001091	0.00641	3.551142	Up	NCK-associated protein 1 like
LAIR1	1.393475593	0.00041	0.003424	3.894699	Up	Leukocyte-associated immunoglobulin-like receptor 1
CD33	1.392716892	0.00015	0.001844	4.238448	Up	CD33 molecule
CCDC141	1.390630771	3.81E–05	0.00081	4.694698	Up	Coiled-coil domain containing 141
TYROBP	1.389702872	0.000536	0.004069	3.801307	Up	TYRO protein tyrosine kinase-binding protein
LINC01279	1.389411419	0.000163	0.001942	4.209992	Up	Long intergenic nonprotein coding RNA 1279
C1QC	1.389318872	0.000497	0.003876	3.827673	Up	Complement C1q C chain
FCGR2B	1.385440012	0.007353	0.024346	2.841262	Up	Fc fragment of IgG receptor IIb
CD6	1.384622356	0.007049	0.023671	2.8578	Up	CD6 molecule
RET	1.383263102	1.16E–06	0.000107	5.835073	Up	Ret proto-oncogene
CD1D	1.379768072	0.001868	0.009323	3.357612	Up	CD1d molecule

(Continued)

Table 1. (Continued)

Gene Symbol	logFC	*p* Value	adj. *p*. Val	t Value	Regulation	Gene Name
TMC3	1.379570249	6.3E–05	0.001085	4.52761	Up	Transmembrane channel-like 3
OSR2	1.378917202	0.000766	0.005079	3.676356	Up	Odd-skipped-related transciption factor 2
CD53	1.37630359	0.002489	0.01138	3.252497	Up	CD53 molecule
CCL13	1.37319011	0.007401	0.024471	2.838721	Up	C-C motif chemokine ligand 13
PLXNA4	1.372503449	1E–05	0.000368	5.132134	Up	Plexin A4
CUX2	1.371842845	0.004435	0.016911	3.036314	Up	Cut-like homeobox 2
DEF6	1.371372718	0.001168	0.00672	3.527002	Up	DEF6 guanine nucleotide exchange factor
ZBP1	1.370641955	0.008335	0.026701	2.791957	Up	Z-DNA-binding protein 1
CD209	1.366297575	0.000818	0.00532	3.653375	Up	CD209 molecule
LCP1	1.365542557	0.00474	0.017702	3.010988	Up	Lymphocyte cytosolic protein 1
DAPP1	1.364139106	0.009696	0.029786	2.731881	Up	Dual adaptor of phosphotyrosine and 3-phosphoinositides 1
LOC101927751	1.362667744	1.13E–05	0.000401	5.093561	Up	Uncharacterized LOC101927751
FAM78A	1.361085133	0.000202	0.002219	4.137502	Up	Family with sequence similarity 78 member A
TMEM119	1.359810238	1.01E–06	0.000101	5.879055	Up	Transmembrane protein 119
CNNM1	1.357575788	7.28E–08	2E–05	6.737948	Up	Cyclin and CBS domain divalent metal cation transport mediator 1
SOWAHD	1.356025266	6.45E–06	0.000286	5.27639	Up	Sosondowahankyrin repeat domain family member D
GLIPR2	1.353584347	0.000118	0.001603	4.318582	Up	GLI pathogenesis-related 2
MYBL2	1.352484041	0.012449	0.035893	2.631173	Up	MYB proto-oncogene-like 2
SPOCD1	1.351281328	0.003548	0.01453	3.120546	Up	SPOC domain containing 1
FOXJ1	1.350490301	3.81E–05	0.00081	4.694772	Up	Forkhead box J1
FOSB	−5.955510598	2.65E–10	4.55E–07	−8.64163	Down	FosB proto-oncogene, AP-1 transcription factor subunit
NR4A1	−4.611444611	2.58E–13	4.44E–09	−11.229	Down	Nuclear receptor subfamily 4 group A member 1
FOS	−4.5121246	1.47E–09	1.6E–06	−8.04524	Down	Fos proto-oncogene, AP-1 transcription factor subunit
NR4A2	−4.07128855	2.95E–12	2.54E–08	−10.2819	Down	Nuclear receptor subfamily 4 group A member 2
EGR1	−4.024708778	4.56E–10	6.54E–07	−8.45074	Down	Early growth response 1
ATF3	−3.460513164	6.03E–11	2.07E–07	−9.16773	Down	Activating transcription factor 3
NR4A3	−3.232228822	2.2E–11	1.26E–07	−9.53288	Down	Nuclear receptor subfamily 4 group A member 3
KLK1	−3.193634749	0.001507	0.008004	−3.43551	Down	Kallikrein 1
MIR3189	−3.171704968	1.97E–07	3.63E–05	−6.41123	Down	MicroRNA 3189
RGS1	−3.105798597	1.43E–05	0.000463	−5.01731	Down	Regulator of G protein signaling 1
SRRM4	−3.096268137	0.001001	0.006068	−3.582	Down	Serine/arginine repetitive matrix 4
DUSP1	−3.029067693	2.94E–11	1.26E–07	−9.42777	Down	Dual-specificity phosphatase 1
SPDYE7P	−2.73813522	0.002285	0.010712	−3.28396	Down	Speedy/RINGO cell cycle regulator family member E7, pseudogene
RNR1	−2.707745724	4.93E–07	6.57E–05	−6.1119	Down	s-rRNA
FER1L6-AS2	−2.616619977	0.000245	0.002508	−4.07122	Down	FER1L6 antisense RNA 2
HSPA1B	−2.535704377	6.65E–05	0.00112	−4.50986	Down	Heat shock protein family A (Hsp70) member 1B
MIR6883	−2.518589531	6.05E–06	0.000275	−5.29707	Down	MicroRNA 6883
GUCY2EP	−2.500664089	6.49E–06	0.000287	−5.27433	Down	Guanylatecyclase 2E, pseudogene
RNR2	−2.494806379	3.34E–07	5.13E–05	−6.23865	Down	l-rRNA
TRIM50	−2.485748172	0.000418	0.00348	−3.88753	Down	Tripartite motif containing 50
EGR3	−2.427252952	9.27E–07	9.57E–05	−5.90664	Down	Early growth response 3
ZFP36	−2.35906331	4.05E–10	6.32E–07	−8.49276	Down	ZFP36 ring finger protein
FER1L6-AS1	−2.328852892	0.000345	0.003071	−3.95409	Down	FER1L6 antisense RNA 1
TRPM6	−2.278882664	0.000406	0.003405	−3.8979	Down	Transient receptor potential cation channel subfamily M member 6
GC	−2.250800387	0.004612	0.017369	−3.02138	Down	GC vitamin D-binding protein
LOC101927136	−2.248315905	0.003123	0.013244	−3.16829	Down	Uncharacterized LOC101927136
MIR6863	−2.197414848	0.001621	0.008432	−3.40906	Down	MicroRNA 6863
HMGN5	−2.189083582	2.7E–05	0.000658	−4.80822	Down	High-mobility group nucleosome-binding domain 5

(Continued)

Table 1. (Continued)

Gene Symbol	logFC	*p* Value	adj. *p*. Val	t Value	Regulation	Gene Name
IGFBP1	−2.15887204	0.000581	0.004293	−3.77361	Down	Insulin-like growth factor-binding protein 1
CR2	−2.129234349	0.001065	0.006322	−3.55983	Down	Complement C3d receptor 2
G6PC	−2.118802858	9.29E–05	0.001369	−4.39837	Down	Glucose-6-phosphatase catalytic subunit
ADAMTS4	−2.110266039	0.000362	0.00316	−3.93773	Down	ADAM metallopeptidase with thrombospondin-type 1 motif 4
PDK4	−2.080535916	1.16E–07	2.73E–05	−6.58537	Down	Pyruvate dehydrogenase kinase 4
ANKRD20A8P	−2.075914128	0.011979	0.034855	−2.64681	Down	Ankyrin repeat domain 20 family member A8, pseudogene
ASB15	−2.074273921	0.002705	0.012016	−3.22167	Down	Ankyrin repeat and SOCS box containing 15
FMN2	−2.07242757	0.000186	0.002119	−4.16515	Down	Formin 2
NDNF	−2.064839947	0.001193	0.006826	−3.51938	Down	Neuron-derived neurotrophic factor
C11orf87	−2.041720603	0.015216	0.04155	−2.54887	Down	Chromosome 11 open reading frame 87
ALB	−2.030814176	0.013963	0.038958	−2.58426	Down	Albumin
TNS4	−2.020912368	0.00012	0.001625	−4.31117	Down	Tensin 4
SLCO4A1-AS1	−2.019564941	2.06E–05	0.000555	−4.89754	Down	SLCO4A1 antisense RNA 1
LINC00473	−2.010041324	3.61E–06	0.000202	−5.4648	Down	Long intergenic nonprotein coding RNA 473
PCAT29	−2.003351434	0.000531	0.004056	−3.80455	Down	Prostate cancer-associated transcript 29
MUC13	−1.995102383	0.008157	0.026293	−2.80048	Down	Mucin 13, cell surface associated
JUNB	−1.991633705	5.39E–07	7.02E–05	−6.08312	Down	JunB proto-oncogene, AP-1 transcription factor subunit
JUN	−1.986246749	1.34E–07	2.92E–05	−6.53681	Down	Jun proto-oncogene, AP-1 transcription factor subunit
OR2T3	−1.98213864	0.001662	0.008571	−3.39995	Down	Olfactory receptor family 2 subfamily T member 3
GDF15	−1.981447549	1.02E–07	2.58E–05	−6.62662	Down	Growth differentiation factor 15
LOC221946	−1.970485542	2.39E–05	0.000609	−4.84741	Down	Uncharacterized LOC221946
CYP26B1	−1.970209556	2.75E–06	0.000178	−5.55309	Down	Cytochrome P450 family 26 subfamily B member 1
USP32P1	−1.950033841	0.009155	0.028541	−2.75476	Down	Ubiquitin-specific peptidase 32 pseudogene 1
HELT	−1.943146021	0.001919	0.009527	−3.34782	Down	HeltbHLH transcription factor
DUSP2	−1.940947917	4.5E–06	0.00023	−5.39361	Down	Dual-specificity phosphatase 2
LOC101928596	−1.922413251	0.002039	0.00991	−3.32563	Down	Uncharacterized LOC101928596
SLC2A3	−1.921295543	6.97E–07	8.04E–05	−5.99957	Down	Solute carrier family 2 member 3
HRG	−1.916581752	2.88E–05	0.000684	−4.78697	Down	Histidine-rich glycoprotein
CCL3	−1.908749902	0.000502	0.003895	−3.82424	Down	C–C motif chemokine ligand 3
GPRC6A	−1.892233354	0.007065	0.023712	−2.85689	Down	G protein-coupled receptor class C group 6 member A
PTHLH	−1.892185067	4.03E–05	0.000839	−4.67555	Down	Parathyroid hormone-like hormone
APOH	−1.882195391	0.003778	0.015145	−3.0969	Down	Apolipoprotein H
HCRTR2	−1.872393755	0.016192	0.043468	−2.52311	Down	Hypocretin receptor 2
OR2T34	−1.871067826	0.016529	0.044172	−2.51455	Down	Olfactory receptor family 2 subfamily T member 34
CALB1	−1.870574756	0.001601	0.008364	−3.41362	Down	Calbindin 1
AKR1B10	−1.868181241	0.001527	0.008088	−3.4306	Down	Aldo-ketoreductase family 1 member B10
EGF	−1.867644284	0.00043	0.00354	−3.8782	Down	Epidermal growth factor
TCF24	−1.863801103	0.000503	0.003901	−3.82323	Down	Transcription factor 24
CRABP1	−1.860745898	0.003988	0.015702	−3.07657	Down	Cellular retinoic acid-binding protein 1
FLJ31356	−1.857719719	2.29E–09	2.07E–06	−7.89515	Down	Uncharacterized protein FLJ31356
LINC00417	−1.854558477	0.018016	0.047092	−2.47855	Down	Long intergenic nonprotein coding RNA 417
GRIA2	−1.852599065	0.000777	0.005137	−3.67139	Down	Glutamate ionotropic receptor AMPA-type subunit 2
CYP27B1	−1.850938356	5.07E–05	0.00096	−4.60016	Down	Cytochrome P450 family 27 subfamily B member 1
LINC01230	−1.845553648	0.000183	0.002096	−4.16956	Down	Long intergenic nonprotein coding RNA 1230
PDZK1P1	−1.844160787	0.017724	0.046497	−2.48539	Down	PDZ domain containing 1 pseudogene 1
NR0B2	−1.838257029	8.06E–08	2.13E–05	−6.70418	Down	Nuclear receptor subfamily 0 group B member 2
GAD1	−1.833958519	0.000135	0.001736	−4.27343	Down	Glutamate decarboxylase 1
LINC01847	−1.823778057	0.00251	0.011445	−3.24929	Down	Long intergenic nonprotein coding RNA 1847
OR2T35	−1.817496772	0.017342	0.045801	−2.49452	Down	Olfactory receptor family 2 subfamily T member 35

(Continued)

Table 1. (Continued)

Gene Symbol	logFC	*p* Value	adj. *p*. Val	t Value	Regulation	Gene Name
DDN	−1.816515681	0.003369	0.014028	−3.13991	Down	Dendrin
OSM	−1.809974482	4.5E–06	0.00023	−5.39347	Down	Oncostatin M
SLC12A3	−1.806889876	0.012697	0.036365	−2.62312	Down	Solute carrier family 12 member 3
CXXC4-AS1	−1.802551841	0.00107	0.00634	−3.55823	Down	CXXC4 antisense RNA 1
LINC01485	−1.801532434	6.62E–05	0.001118	−4.51152	Down	Long intergenic nonprotein coding RNA 1485
CEL	−1.791647114	0.000873	0.005536	−3.63032	Down	Carboxyl ester lipase
ESM1	−1.788028034	7.6E–05	0.001229	−4.46553	Down	Endothelial cell-specific molecule 1
FOXF1	−1.778554943	5.07E–08	1.56E–05	−6.85704	Down	Forkhead box F1
CHI3L1	−1.760426944	3.27E–05	0.000735	−4.74521	Down	Chitinase 3-like 1
NPHS1	−1.75953731	0.008924	0.028045	−2.76491	Down	NPHS1 adhesion molecule, nephrin
EGR2	−1.752584545	0.000609	0.004415	−3.75721	Down	Early growth response 2
NPTX1	−1.748040947	1.22E–05	0.000417	−5.06751	Down	Neuronal pentraxin 1
LINC00323	−1.744409028	0.001604	0.008375	−3.41293	Down	Long intergenic nonprotein coding RNA 323
GADD45B	−1.740349827	1.42E–09	1.6E–06	−8.05874	Down	Growth arrest and DNA damage-inducible beta
CXCL2	−1.739324966	0.000318	0.002912	−3.98137	Down	C-X-C motif chemokine ligand 2
ZNF804B	−1.733201555	9.34E–05	0.001373	−4.39665	Down	Zinc finger protein 804B
DLGAP2	−1.730447868	0.0016	0.008363	−3.41377	Down	DLG-associated protein 2
MRO	−1.729448908	0.000333	0.003003	−3.96617	Down	Maestro
CHP2	−1.728672056	0.016389	0.043895	−2.51807	Down	Calcineurin-like EF-hand protein 2
SNTG1	−1.725236976	0.003801	0.015206	−3.09469	Down	Syntrophin gamma 1
TMIGD1	−1.723453536	0.008318	0.026653	−2.79275	Down	Transmembrane and immunoglobulin domain containing 1
ERRFI1	−1.719155426	1.68E–05	0.000503	−4.96349	Down	ERBB receptor feedback inhibitor 1
MIR23A	−1.698259296	8.39E–06	0.000334	−5.19076	Down	MicroRNA 23a
AFM	−1.697646678	0.006984	0.023513	−2.86141	Down	Afamin
GSTA2	−1.695005472	0.007146	0.023905	−2.85243	Down	Glutathione S-transferase alpha 2
ARC	−1.691564852	4.64E–05	0.000911	−4.62913	Down	Activity regulated cytoskeleton-associated protein
PCK1	−1.687669067	9.55E–05	0.001392	−4.38911	Down	Phosphoenolpyruvatecarboxykinase 1
MRLN	−1.684067815	0.012325	0.035628	−2.63525	Down	Myoregulin
OR2G6	−1.682846251	0.014103	0.039247	−2.58017	Down	Olfactory receptor family 2 subfamily G member 6
MIR554	−1.682490199	1.71E–07	3.31E–05	−6.45693	Down	MicroRNA 554
GJA3	−1.680981251	0.000638	0.00454	−3.74053	Down	Gap junction protein alpha 3
OR2T2	−1.680340426	0.005838	0.020664	−2.93098	Down	Olfactory receptor family 2 subfamily T member 2
GADL1	−1.679083154	0.017945	0.046941	−2.48021	Down	Glutamate decarboxylase-like 1
LINC00964	−1.673915031	0.000814	0.005305	−3.65509	Down	Long intergenic nonprotein coding RNA 964
GSTA7P	−1.670788343	0.013855	0.038725	−2.58746	Down	Glutathione S-transferase alpha 7, pseudogene
CCDC144A	−1.663249282	0.001157	0.00669	−3.5302	Down	Coiled-coil domain containing 144A
SLC28A2	−1.658633673	0.00269	0.011965	−3.22376	Down	Solute carrier family 28 member 2
SCN1A	−1.657619336	0.013168	0.037321	−2.60828	Down	Sodium voltage-gated channel alpha subunit 1
CTSV	−1.652642893	0.000297	0.002803	−4.00501	Down	Cathepsin V
KRTAP5-8	−1.652501654	2.46E–05	0.000618	−4.83842	Down	Keratin-associated protein 5-8
CYP4Z1	−1.650835392	0.000435	0.003558	−3.8736	Down	Cytochrome P450 family 4 subfamily Z member 1
IP6K3	−1.648838717	0.000132	0.001717	−4.28066	Down	Inositol hexakisphosphate kinase 3
DRAIC	−1.636089665	0.000709	0.00483	−3.70347	Down	Downregulated RNA in cancer, inhibitor of cell invasion and migration
GPAT3	−1.631414454	4.15E–06	0.000221	−5.41942	Down	Glycerol-3-phosphate acyltransferase 3
CYP3A7	−1.62542705	0.000397	0.003363	−3.90515	Down	Cytochrome P450 family 3 subfamily A member 7
IL6	−1.625295765	0.01589	0.042893	−2.53091	Down	Interleukin 6
MAFF	−1.613761879	2.32E–05	0.000598	−4.85721	Down	Maf bZIP transcription factor F
SALL3	−1.605351285	0.007947	0.02578	−2.81075	Down	Spalt-like transcription factor 3
APOC3	−1.59993261	0.011819	0.034571	−2.65224	Down	Apolipoprotein C3
IGF2	−1.59274691	0.002899	0.012559	−3.19605	Down	Insulin-like growth factor 2
ETNPPL	−1.591241057	0.011421	0.033757	−2.6661	Down	Ethanolamine-phosphate phospholyase

(Continued)

Table 1. (Continued)

Gene Symbol	logFC	*p* Value	adj. *p*. Val	t Value	Regulation	Gene Name
SYCP2	−1.58976625	2.36E–05	0.000603	−4.85205	Down	Synaptonemal complex protein 2
HPGD	−1.586552352	5.24E–05	0.000978	−4.5893	Down	15-Hydroxyprostaglandin dehydrogenase
ZNF99	−1.580422848	0.00306	0.013042	−3.17586	Down	Zinc finger protein 99
SLC6A17	−1.577887812	2.66E–05	0.000652	−4.81243	Down	Solute carrier family 6 member 17
POM121L1P	−1.55230685	0.003831	0.015294	−3.09164	Down	POM121 transmembranenucleoporin-like 1, pseudogene
MYCNOS	−1.548456266	0.017829	0.046709	−2.48293	Down	MYCN opposite strand
DPP6	−1.546923933	9.24E–05	0.001364	−4.40008	Down	Dipeptidyl peptidase-like 6
TRIM72	−1.545789372	0.002475	0.011332	−3.25453	Down	Tripartite motif containing 72
ADAMTS19	−1.540077561	0.001649	0.008522	−3.4029	Down	ADAM metallopeptidase with thrombospondin type 1 motif 19
OLIG2	−1.539877622	0.000751	0.005004	−3.6836	Down	Oligodendrocyte transcription factor 2
GPR3	−1.535389568	5.22E–05	0.000977	−4.59009	Down	G protein-coupled receptor 3
KCNG3	−1.533543431	5.61E–06	0.000262	−5.32192	Down	Potassium voltage-gated channel modifier subfamily G member 3
PCDH15	−1.528198692	0.003807	0.015226	−3.09408	Down	Protocadherin-related 15
MIR324	−1.527392763	1.45E–05	0.000467	−5.01124	Down	Microrna 324
PYY	−1.525114023	6.1E–05	0.001072	−4.53874	Down	Peptide YY
MIR27A	−1.524858329	0.00249	0.011382	−3.25223	Down	Microrna 27a
LOC200772	−1.518032268	0.008823	0.027862	−2.76944	Down	Uncharacterized LOC200772
SLC36A2	−1.51053746	0.00138	0.00752	−3.4672	Down	Solute carrier family 36 member 2
LMX1B	−1.507775955	0.000483	0.003807	−3.83796	Down	LIM homeobox transcription factor 1 beta
PROZ	−1.49926114	0.001739	0.008872	−3.38355	Down	Protein Z, vitamin K-dependent plasma glycoprotein
PM20D1	−1.499147315	0.003745	0.015053	−3.10025	Down	Peptidase M20 domain containing 1
SLC10A5	−1.498680927	0.000145	0.001808	−4.24972	Down	Solute carrier family 10 member 5
FAM3D	−1.498398868	0.001402	0.007614	−3.46151	Down	Family with sequence similarity 3 member D
CTD-3080P12.3	−1.496303721	0.002033	0.009904	−3.32665	Down	Uncharacterized LOC101928857
CNTNAP5	−1.494811619	0.000399	0.003368	−3.90354	Down	Contactin-associated protein-like 5
LRRC9	−1.494187097	0.001203	0.006851	−3.51629	Down	Leucine-rich repeat containing 9
RHCG	−1.491537913	0.003448	0.014249	−3.13125	Down	Rh family C glycoprotein
TEX41	−1.485020132	2.23E–07	3.79E–05	−6.37087	Down	Testis expressed 41
PADI4	−1.480083711	0.014223	0.039483	−2.5767	Down	Peptidyl arginine deiminase 4
DEPDC7	−1.476291247	4.17E–06	0.000221	−5.41811	Down	DEP domain containing 7
PCOLCE2	−1.474650367	0.00486	0.01802	−3.00145	Down	procollagen C-endopeptidase enhancer 2
TINCR	−1.47186623	0.000968	0.005929	−3.59385	Down	TINCR ubiquitin domain containing
MRPL23-AS1	−1.471655339	0.000456	0.003664	−3.85753	Down	MRPL23 antisense RNA 1
SYT10	−1.470400281	6.59E–05	0.001114	−4.513	Down	Synaptotagmin 10
CREB3L3	−1.467664347	0.012078	0.035068	−2.64347	Down	cAMP-responsive element-binding protein 3 like 3
KIRREL2	−1.461511269	0.002708	0.012016	−3.22124	Down	Kirre-like nephrin family adhesion molecule 2
TMEM200C	−1.45510721	0.000122	0.001641	−4.30616	Down	Transmembrane protein 200C
LOC101929420	−1.452843085	0.006518	0.02238	−2.8883	Down	Uncharacterized LOC101929420
NXPH2	−1.451460309	0.000823	0.005333	−3.65128	Down	Neurexophilin 2
FER1L6	−1.450756096	0.006851	0.023185	−2.8689	Down	Fer-1-like family member 6
CBARP	−1.449743026	2.35E–05	0.000601	−4.85428	Down	CACN subunit beta-associated regulatory protein
LINC01108	−1.448256508	0.000325	0.002945	−3.97448	Down	Long intergenic nonprotein coding RNA 1108
LINC00113	−1.437692624	0.001796	0.009076	−3.37195	Down	Long intergenic nonprotein coding RNA 113
DEPDC1B	−1.43627513	5.2E–06	0.000251	−5.34633	Down	DEP domain containing 1B
BTG2	−1.434897848	1E–06	0.000101	−5.8821	Down	BTG antiproliferation factor 2
IHH	−1.434489782	1.07E–06	0.000104	−5.85878	Down	Indian hedgehog signaling molecule
SNORD97	−1.429953225	3.04E–07	4.75E–05	−6.26958	Down	Small nucleolar RNA, C/D box 97
NPIPB5	−1.429567404	9.75E–05	0.001414	−4.38215	Down	Nuclear pore complex interacting protein family member B5
MIR1914	−1.429519419	0.001069	0.006336	−3.55857	Down	MicroRNA 1914

(Continued)

Table 1. (Continued)

Gene Symbol	logFC	*p* Value	adj. *p*. Val	t Value	Regulation	Gene Name
LINC00871	−1.428825981	0.002081	0.010038	−3.31816	Down	Long intergenic nonprotein coding RNA 871
LOC105375787	−1.422740636	1.2E–06	0.00011	−5.82292	Down	Uncharacterized LOC105375787
RGPD3	−1.421537521	0.013983	0.038995	−2.58368	Down	RANBP2-like and GRIP domain containing 3
MEAT6	−1.418362976	0.01364	0.038298	−2.59385	Down	Melanoma-associated transcript 6
LPA	−1.411967686	0.00184	0.009223	−3.36313	Down	Lipoprotein(a)
CA8	−1.40998739	6.44E–09	4.26E–06	−7.54447	Down	Carbonic anhydrase 8
TMEM207	−1.409127764	0.003564	0.014563	−3.11884	Down	Transmembrane protein 207
CYP4F2	−1.408088156	0.005401	0.019466	−2.96097	Down	Cytochrome P450 family 4 subfamily F member 2
PLCE1-AS1	−1.406613355	2.74E–05	0.000663	−4.8028	Down	PLCE1 antisense RNA 1
PTGER3	−1.40433875	2.43E–06	0.000168	−5.5942	Down	Prostaglandin E receptor 3
SERPINA4	−1.403113302	0.000123	0.001651	−4.30327	Down	Serpin family A member 4
LOC100129316	−1.39444782	0.000316	0.002903	−3.98426	Down	Uncharacterized LOC100129316
FOLH1B	−1.390460703	0.003747	0.015059	−3.1	Down	Folate hydrolase 1B
LINC01055	−1.38058556	0.012987	0.036968	−2.61392	Down	Long intergenic nonprotein coding RNA 1055
L3MBTL4-AS1	−1.37580076	1.5E–06	0.000125	−5.75109	Down	L3MBTL4 antisense RNA 1
SLC26A4	−1.372335672	0.011834	0.034591	−2.65173	Down	Solute carrier family 26 member 4
CTSLP8	−1.370209572	0.008179	0.026331	−2.79939	Down	Cathepsin L pseudogene 8
PER1	−1.362768075	3.16E–05	0.000724	−4.75616	Down	Period circadian regulator 1
WT1	−1.362438811	0.001653	0.008535	−3.40193	Down	WT1 transcription factor
GPR26	−1.361155893	0.000652	0.004606	−3.73289	Down	G protein-coupled receptor 26
HCN2	−1.358872972	1.82E–05	0.000524	−4.93725	Down	Hyperpolarization-activated cyclic nucleotide-gated potassium and sodium channel 2
LGSN	−1.35743098	0.002526	0.011496	−3.24697	Down	Lengsin, lens protein with glutamine synthetase domain
ABCC11	−1.35662988	0.017397	0.045878	−2.4932	Down	ATP-binding cassette subfamily C member 11
LINC01060	−1.354954664	0.004572	0.017281	−3.02468	Down	Long intergenic nonprotein coding RNA 1060
CDH20	−1.354557464	0.011483	0.03388	−2.66394	Down	Cadherin 20
PLCZ1	−1.354493222	0.000204	0.002231	−4.13326	Down	Phospholipase C zeta 1
PLEKHD1	−1.353951429	0.013036	0.03706	−2.61238	Down	Pleckstrin homology and coiled-coil domain containing D1
FBN3	−1.353146437	0.000356	0.003126	−3.94334	Down	Fibrillin 3
LINC00484	−1.347121178	9.63E–05	0.001402	−4.3864	Down	Long intergenic nonprotein coding RNA 484
APOB	−1.346767222	0.000868	0.005514	−3.63257	Down	Apolipoprotein B
APOLD1	−1.337981834	6.75E–05	0.001131	−4.50472	Down	Apolipoprotein L domain containing 1
PLPPR4	−1.335848132	0.001491	0.007939	−3.43935	Down	Phospholipid phosphatase-related 4
FCN2	−1.334678426	0.000506	0.003913	−3.82162	Down	Ficolin 2
RASD1	−1.33165582	0.00329	0.013774	−3.14879	Down	Ras-related dexamethasone-induced 1
ATOH7	−1.330889316	0.017065	0.045275	−2.50123	Down	Atonal bHLH transcription factor 7
CXCL3	−1.330777415	0.001736	0.008867	−3.38419	Down	C-X-C motif chemokine ligand 3
TCEAL2	−1.329162032	2.26E–05	0.000588	−4.8665	Down	Transcription elongation factor A-like 2
ALDH1L1-AS1	−1.32788233	0.000679	0.004714	−3.7189	Down	ALDH1L1 antisense RNA 1
SLC26A7	−1.32309366	9.51E–05	0.00139	−4.39044	Down	Solute carrier family 26 member 7
CYP2C8	−1.317744251	0.000385	0.003288	−3.91645	Down	Cytochrome P450 family 2 subfamily C member 8
LINC00645	−1.317115448	4.76E–05	0.000926	−4.62111	Down	Long intergenic nonprotein coding RNA 645
OLR1	−1.315145688	4.1E–06	0.00022	−5.4239	Down	Oxidized low-density lipoprotein receptor 1
NTNG1	−1.313556498	0.0038	0.015206	−3.09475	Down	Netrin G1
MROH5	−1.311546405	0.001098	0.006437	−3.549	Down	Maestro heat-like repeat family member 5 (gene/pseudogene)
SNORA63	−1.309234838	5.18E–05	0.000974	−4.59258	Down	Small nucleolar RNA, H/ACA box 63
C1QL1	−1.308178806	0.010298	0.031187	−2.70779	Down	Complement C1q-like 1
SLC8A1-AS1	−1.305938873	2.03E–05	0.000552	−4.90087	Down	SLC8A1 antisense RNA 1
TREM1	−1.304718012	0.016142	0.043381	−2.52439	Down	Triggering receptor expressed on myeloid cells 1
FOXI2	−1.304685736	0.003445	0.014249	−3.13157	Down	Forkhead box I2
PVALB	−1.304363429	0.002758	0.012155	−3.21449	Down	Parvalbumin

(Continued)

Table 1. (Continued)

Gene Symbol	logFC	*p* Value	adj. *p*. Val	t Value	Regulation	Gene Name
LOC101927318	−1.303237273	0.00023	0.00241	−4.09201	Down	Uncharacterized LOC101927318
GABRA2	−1.295486714	0.000679	0.004714	−3.71874	Down	Gamma-aminobutyric acid type A receptor alpha2 subunit
TMEM52B	−1.29520852	0.000201	0.002215	−4.13894	Down	Transmembrane protein 52B
ATP6V0D2	−1.292251566	0.000684	0.004733	−3.71608	Down	ATPase H + transporting V0 subunit d2
ATP6V1G3	−1.291903527	0.000874	0.005538	−3.62997	Down	ATPase H + transporting V1 subunit G3
CSRNP1	−1.290344053	1.7E–08	7.67E–06	−7.21996	Down	Cysteine- and serine-rich nuclear protein 1
LINC01450	−1.289799129	0.000668	0.004664	−3.72476	Down	Long intergenic nonprotein coding RNA 1450
SLC4A1	−1.289449946	0.004603	0.01736	−3.02212	Down	Solute carrier family 4 member 1 (Diego blood group)
LOC101060553	−1.28899537	0.000157	0.001908	−4.22131	Down	Uncharacterized LOC101060553
MIR3183	−1.288700614	0.005356	0.01932	−2.96417	Down	microRNA 3183
GPC5	−1.288623288	0.014826	0.040723	−2.5596	Down	Glypican 5
MME	−1.288378854	0.000993	0.006035	−3.58459	Down	Membrane metalloendopeptidase
ACOT12	−1.286412523	0.000889	0.005604	−3.62385	Down	Acyl-CoA thioesterase 12
MGAM2	−1.285372755	2.29E–05	0.000592	−4.86206	Down	Maltase-glucoamylase 2 (putative)
BPI	−1.283621874	0.016984	0.045107	−2.50323	Down	Bactericidal permeability-increasing protein
PTPRO	−1.283576103	0.001941	0.009605	−3.3436	Down	Protein tyrosine phosphatase receptor type O
RGS7	−1.280998045	0.002118	0.01016	−3.31169	Down	Regulator of G protein signaling 7
COL6A4P2	−1.280622568	0.00095	0.005853	−3.60062	Down	Collagen type VI alpha 4 pseudogene 2
F2RL3	−1.279685417	0.00089	0.005607	−3.62345	Down	F2R-like thrombin or trypsin receptor 3
CYP3A4	−1.279617141	0.000116	0.00159	−4.3231	Down	Cytochrome P450 family 3 subfamily A member 4
LINC00970	−1.275581109	0.001008	0.006094	−3.57936	Down	Long intergenic nonprotein coding RNA 970
CACNB4	−1.275043635	2.68E–05	0.000654	−4.81055	Down	Calcium voltage-gated channel auxiliary subunit beta 4
CALCR	−1.275036739	4.23E–05	0.000865	−4.65987	Down	Calcitonin receptor
LSMEM1	−1.274783777	2.29E–07	3.81E–05	−6.3619	Down	Leucine-rich single-pass membrane protein 1
UGT2B7	−1.273593035	0.001156	0.006683	−3.53073	Down	UDP glucuronosyltransferase family 2 member B7
MTTP	−1.271212874	0.00091	0.005672	−3.61577	Down	Microsomal triglyceride transfer protein
CYP4A11	−1.269785869	0.000883	0.005577	−3.62621	Down	Cytochrome P450 family 4 subfamily A member 11
CHRM3-AS2	−1.269628975	9.73E–05	0.001413	−4.38283	Down	CHRM3 antisense RNA 2
DMRT2	−1.266816699	4.09E–05	0.000847	−4.67098	Down	Doublesex and mab-3-related transcription factor 2
RGS16	−1.26587407	4.23E–06	0.000223	−5.41333	Down	Regulator of G protein signaling 16
STPG3-AS1	−1.264596788	0.000381	0.00326	−3.92013	Down	STPG3 antisense RNA 1
ADAMTS17	−1.264266059	7.2E–05	0.001176	−4.48351	Down	ADAM metallopeptidase with thrombospondin type 1 motif 17
STRA6	−1.262382386	0.010303	0.031193	−2.70757	Down	Stimulated by retinoic acid 6
IFIT1B	−1.261998139	0.000918	0.005705	−3.61259	Down	Interferon-induced protein with tetratricopeptide repeats 1B
LINC00482	−1.261995523	0.006582	0.022517	−2.88453	Down	Long intergenic nonprotein coding RNA 482
PPP2R2C	−1.261940465	0.003244	0.013629	−3.15411	Down	Protein phosphatase 2 regulatory subunit Bgamma
STPG3	−1.261181245	0.000552	0.00415	−3.79133	Down	Sperm-tail PG-rich repeat containing 3
ZYG11A	−1.260941533	0.00695	0.023444	−2.86332	Down	Zyg-11 family member A, cell cycle regulator
CDC20B	−1.259551185	0.009685	0.029778	−2.73233	Down	Cell division cycle 20B
ZNF732	−1.258545333	0.002227	0.010535	−3.29339	Down	Zinc finger protein 732
XPNPEP2	−1.251978507	0.000984	0.006001	−3.58806	Down	X-prolylaminopeptidase 2
NUGGC	−1.251480291	0.000372	0.003217	−3.92756	Down	Nuclear GTPase, germinal center associated
UCN3	−1.250096089	0.004835	0.017961	−3.00339	Down	Urocortin 3
MUC5B	−1.248150313	0.001809	0.009105	−3.36931	Down	Mucin 5B, oligomeric mucus/gel-forming
FAM151A	−1.247526187	0.011061	0.032948	−2.67903	Down	Family with sequence similarity 151 member A
LOC101928911	−1.247448929	0.003556	0.014541	−3.11966	Down	Uncharacterized LOC101928911
F3	−1.245936124	0.000125	0.001663	−4.29908	Down	Coagulation factor III, tissue factor

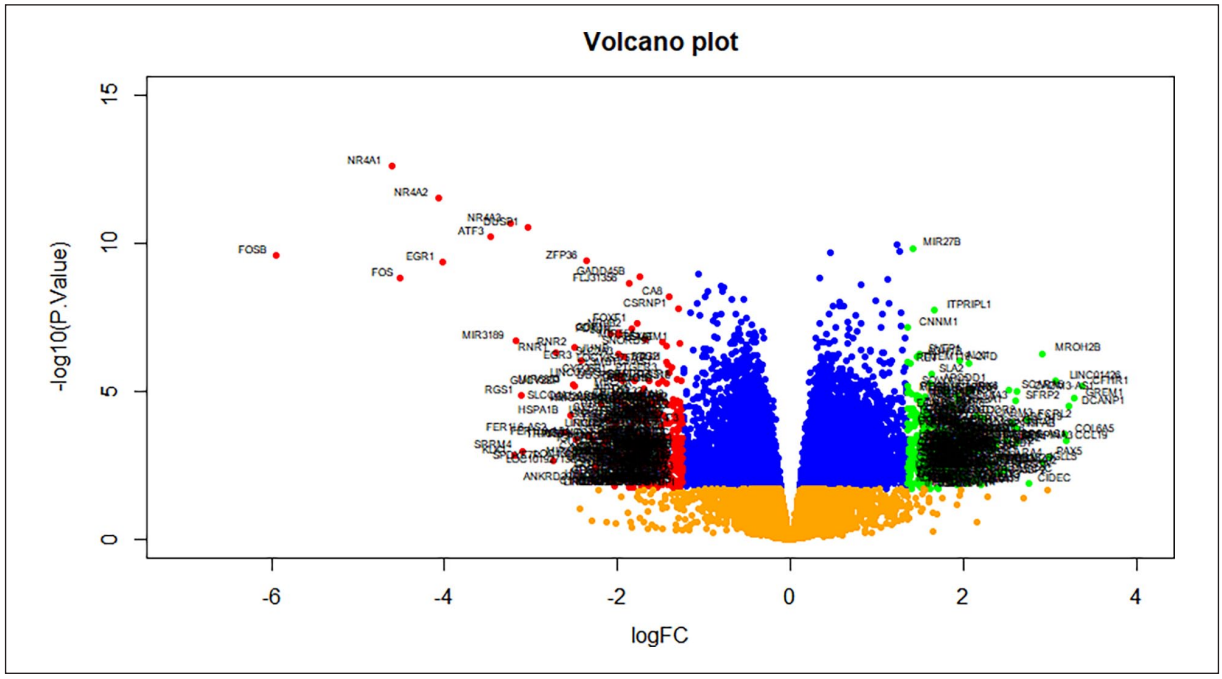

Figure 1. Volcano plot of differentially expressed genes.
Genes with a significant change of more than two-fold were selected. Green dot represented upregulated significant genes and the red dot represented downregulated significant genes.

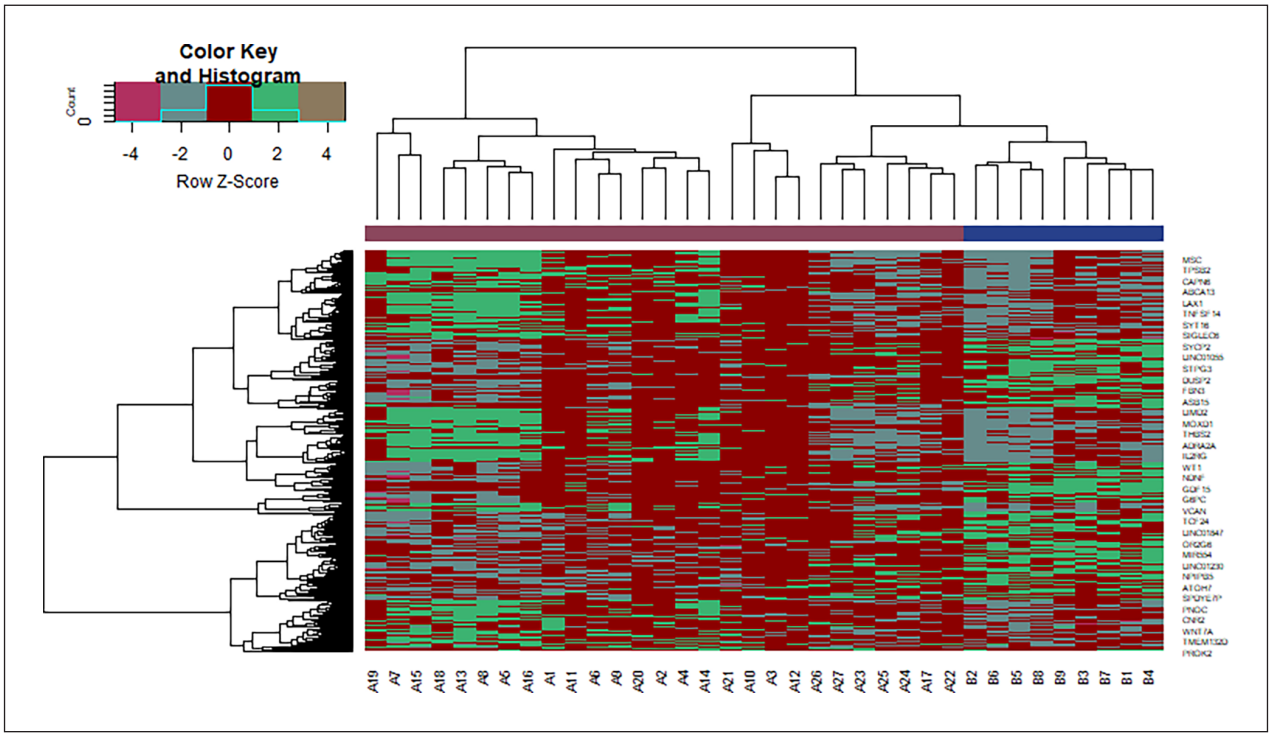

Figure 2. Heat map of differentially expressed genes.
Legend on the top left indicate log fold change of genes. (A1–A28 = DN samples; B1–B9 = normal control samples).

Table 2. The enriched GO terms of the up- and down-regulated differentially expressed genes.

GO ID	CATEGORY	GO Name	*p* Value	FDR B&H	FDR B&Y	Bonferroni	Gene Count	Gene
Upregulated genes								
GO:0001775	BP	Cell activation	9.81E–44	3.95E–40	3.51E–39	3.95E–40	98	SERPINA3, CD244, TNFSF14, MZB1, ABCA13, IRF4, IKZF1, TNFRSF18, MDK, ITGAD, UBASH3A, ITGAL, SIT1, JAML, IGLL5, TESPA1, CD209, LAX1, PLAC8, SIRPG, EOMES, CD84, CCR2, TYROBP, CFD, SAA1, ADRA2A, FCRL1, FCRL3, FCER1A, MS4A2, FCGR2B, SASH3, BTK, GRAP2, C1QA, C3, SLA2, CCL19, CCL21, ALOX5, CNR2, RAC2, COL1A1, COL1A2, FOXJ1, COL3A1, DOCK2, IKZF3, THEMIS, CARMIL2, COMP, WNT7A, LAIR1, ARHGAP9, LCK, LCN2, LCP1, SLAMF1, CD1C, RHOH, CORO1A, MIR142, CD1D, CD2, CD3D, CD3E, CD3G, CD6, CD7, CD8A, PIK3R6, TIGIT, CD19, MS4A1, TIMP1, CD33, PYCARD, SLPI, CD48, CD53, PRKCB, CD79A, CD79B, CARD11, LTF, SLAMF7, LY9, CD180, FUT7, LYZ, CTSG, IL2RB, IL2RG, CLEC4C, TREML2, NCKAP1L
GO:0002682	BP	Regulation of immune system process	2.49E–36	3.34E–33	2.96E–32	1.00E–32	95	MYO1G, CFHR1, CD244, TNFSF14, MZB1, REG3G, GPR55, IRF4, IKZF1, TNFRSF18, MDK, UBASH3A, ITGAL, SIT1, JAML, IGLL5, TESPA1, CD209, LAX1, SIRPG, BLK, CD84, CCR2, ZBP1, TYROBP, CFD, FCRL3, FCER1A, MS4A2, FCER2, TRAT1, FCGR2B, SASH3, BTK, GRAP2, XCL2, C1QA, C1QC, C1R, C1S, C3, SLA2, CCL19, CCL21, CLEC10A, CNR2, RAC2, COL1A1, COL1A2, FOXJ1, COL3A1, CXCR3, IKZF3, THEMIS, CARMIL2, LAIR1, LCK, SLAMF1, CD200R1, TLR10, CD1C, CORO1A, MIR142, CD1D, CD1E, CD2, CD3D, CD3E, CD3G, CD247, CD5L, CD6, CD8A, PIK3R6, TIGIT, CD19, MS4A1, CD33, PYCARD, CD48, PRKCB, CD79A, CD79B, CARD11, PAX5, GREM1, LTF, SLAMF7, SH2D1A, CTSG, IL2RG, CLEC4C, TREML2, LILRA4, NCKAP1L
GO:0009986	CC	Cell surface	4.78E–24	1.92E–21	1.26E–20	1.92E–21	60	FCRL2, CRLF1, CD244, TNFRSF18, ITGAD, ITGAL, IGLL5, ITGB6, CD209, ADCYAP1R1, CCR2, TYROBP, ITGBL1, FAP, FCRL1, FCRL3, FCER1A, MS4A2, FCER2, FCGR2B, NTM, C3, CCR5, MMP7, ISLR2, CXCR3, WNT7A, WNT7B, SLAMF1, CD200R1, CD1C, CD1D, CD1E, CD2, CD3D, CD3E, CD3G, CD5L, CD6, CD8A, TIGIT, CD19, MS4A1, SCARA5, CD33, VCAN, CD48, CD53, CD79A, CD79B, GREM1, LTF, FCRL5, SLAMF7, LY9, CTSG, IL2RB, IL2RG, TREML2, FCMR
GO:0031226	CC	Intrinsic component of plasma membrane	9.46E–11	6.34E–09	4.17E–08	3.80E–08	56	CADM3, CD52, APCDD1, GPR55, TNFRSF18, ITGAD, ITGAL, SIT1, TMC3, ITGB6, ADCYAP1R1, CD84, CCR2, TYROBP, ITGBL1, ADRA2A, KCNA3, FCER1A, MS4A2, FCER2, TRAT1, FCGR2B, TMC8, KCNS1, CCR5, CNR2, CXCR3, CP, RET, NCMAP, TLR10, KCNV1, CD1C, CD1D, CD1E, CD2, CD3E, CD3G, CD6, CD8A, P2RX5, CD19, MS4A1, SCARA5, CD33, SIGLEC6, PLXNA4, CD48, CD53, CD79B, HAS2, IL2RB, IL2RG, S1PR4, LILRA4, NCKAP1L
GO:0005102	MF	signaling receptor binding	2.49E–09	1.46E–06	1.01E–05	1.46E–06	55	GDF5, CRLF1, CD244, TNFSF14, MDK, JAML, IGLL5, ITGB6, TESPA1, FABP4, BLK, CCR2, TYROBP, ERFE, TUBB3, ITGBL1, FAP, SAA1, ADRA2A, FCER2, TRAT1, PPP1R1B, XCL2, TMC8, C3, CCL13, JAKMIP1, CCL19, CCL21, PNOC, COL3A1, DOCK2, COL5A1, SFRP2, COMP, WNT7A, WNT7B, REG1A, LCK, LCP1, CD1D, CD2, CD3E, CD3G, CD8A, TIGIT, MS4A1, TIMP1, PYCARD, JCHAIN, WNT10A, PRKCB, GREM1, MIR27B, LILRA4
GO:0042802	MF	Identical protein binding	1.11E–05	5.00E–04	3.48E–03	6.50E–03	49	CFHR1, CADM3, GDF5, TPSAB1, TNFSF14, APCDD1, MDFI, JAML, CD84, CCR2, ZBP1, TYROBP, ERFE, FAP, ADRA2A, BTK, C1S, COL1A1, COL1A2, IKZF3, REG1A, TDO2, LCK, LCN2, LCP1, SLAMF1, TLR10, TBX18, SYT16, CORO1A, CD2, CD3D, CD3E, CD3G, CD247, CD6, ALX1, CD8A, TIGIT, PYCARD, JCHAIN, GZMA, GLIPR2, CD79A, CD79B, GREM1, HAS2, SLAMF7, LYZ
Down-regulated genes								
GO:0009725	BP	Response to hormone	1.08E–08	1.59E–05	1.41E–04	4.43E–05	33	PDK4, CYP27B1, PER1, NR4A1, JUN, JUNB, ATP6V1G3, BTG2, HPGD, ATP6V0D2, NR0B2, TRIM72, CALCR, GDF15, FOS, DUSP1, NR4A2, WT1, NR4A3, APOB, APOC3, ZFP36, IGF2, IGFBP1, EGR1, EGR2, ERRFI1, UCN3, IHH, CTSV, PCK1, IL6
GO:0006811	BP	Ion transport	2.72E–06	6.96E–04	6.19E–03	1.11E–02	42	TRPM6, CYP4A11, SLC6A17, SLC26A4, CYP27B1, PER1, CBARP, HCN2, PTGER3, MRLN, SLC36A2, ATP6V1G3, SCN1A, ARC, HRG, CCL3, ATP6V0D2, STRA6, RHCG, DPP6, PLCZ1, CACNB4, CALCR, F2RL3, PM20D1, ABCC11, GRIA2, CYP4F2, APOC3, KCNG3, SYT10, RGS7, SLC4A1, EGF, SLC12A3, SLC26A7, SLC10A5, CHP2, SLC28A2, MTTP, G6PC, GABRA2
GO:0005887	CC	Integral component of plasma membrane	2.15E–04	2.45E–02	1.59E–01	7.91E–02	33	CEL, SLC6A17, SLC26A4, HCN2, PTGER3, GJA3, PLPPR4, PTPRO, SCN1A, PCDH15, GPC5, MME, STRA6, RHCG, NPHS1, GPR3, DPP6, CALCR, F2RL3, ABCC11, GRIA2, GPRC6A, KCNG3, OLR1, SLC2A3, SLC4A1, SLC12A3, SLC26A7, SLC28A2, FOLH1B, IL6, HCRTR2, GABRA2
GO:0000790	CC	Nuclear chromatin	2.99E–02	1.71E–01	1.00E + 00	1.00E + 00	28	SALL3, ATOH7, HELT, NR4A1, CSRNP1, JUN, JUNB, BTG2, MAFF, CREB3L3, NR0B2, FOXF1, FOS, FOSB, NR4A2, WT1, NR4A3, DMRT2, EGR1, EGR2, ZNF732, EGR3, LMX1B, FOXI2, ATF3, ZNF99, OLIG2
GO:0008289	MF	Lipid binding	4.64E–05	6.47E–03	4.61E–02	3.24E–02	22	CEL, CYP3A4, GC, F3, BPI, APOLD1, UGT2B7, ALB, MME, STRA6, TRIM72, PLCZ1, CALB1, CYP26B1, APOB, APOC3, APOH, CRABP1, SYT10, ACOT12, MTTP, MIR27A
GO:0005215	MF	Transporter activity	5.91E–04	2.01E–02	1.43E–01	4.13E–01	30	TRPM6, SLC6A17, SLC26A4, GC, CBARP, HCN2, MRLN, SLC36A2, GJA3, ATP6V1G3, SCN1A, ARC, ATP6V0D2, STRA6, RHCG, DPP6, CACNB4, PM20D1, ABCC11, GRIA2, APOB, KCNG3, SLC2A3, SLC4A1, SLC12A3, SLC26A7, SLC10A5, SLC28A2, MTTP, GABRA2

BP: Biological Process; CC: Cellular Component; MF: Molecular Functions.

Table 3. The enriched pathway terms of the up- and down-regulated differentially expressed genes.

Pathway ID	Pathway Name	*p*-value	FDR B&H	FDR B&Y	Bonferroni	Gene Count	Gene
Upregulated genes							
1269201	Immunoregulatory interactions between a Lymphoid and a non-Lymphoid cell	2.98E–16	1.12E–13	7.31E–13	1.12E–13	21	ITGAL, JAML, FCGR2B, C3, LAIR1, CD200R1, CD1C, CD1D, CD3D, CD3E, CD3G, CD247, CD8A, CD19, CD33, SIGLEC6, SLAMF7, SH2D1A, TREML2, LILRA4
1269203	Innate Immune System	1.37E–09	2.59E–07	1.68E–06	5.17E–07	47	SERPINA3, ABCA13, REG3G, ITGAL, CD209, PLAC8, CCR2, ZBP1, TYROBP, CFD, SAA1, FCER1A, MS4A2, TRAT1, BTK, GRAP2, C1QA, C1QC, C1R, C1S, C3, CLEC10A, ALOX5, DOCK2, LAIR1, ARHGAP9, RET, LCK, LCN2, TLR10, CD3G, CD247, CD19, CD33, PYCARD, GZMM, CD53, CARD11, LTF, CD180, LYZ, CTSG, IL2RB, IL2RG, CLEC4C, NCKAP1L
1270244	Extracellular matrix organization	8.51E–09	1.07E–06	6.97E–06	3.21E–06	20	GDF5, TPSAB1, COL6A5, ITGAD, ITGAL, ITGB6, COL14A1, MMP7, COL1A1, COL1A2, COL3A1, COL5A1, COL6A3, COMP, TNC, CAPN6, LAMC2, TIMP1, VCAN, CTSG
1269171	Adaptive Immune System	1.77E–07	1.56E–05	1.02E–04	6.69E–05	32	ITGAL, JAML, CD209, BLK, TYROBP, TRAT1, FCGR2B, BTK, GRAP2, C3, LAIR1, LCK, CD200R1, CD1C, CD1D, CD3D, CD3E, CD3G, CD247, CD8A, CD19, CD33, SIGLEC6, DAPP1, PRKCB, CD79A, CD79B, CARD11, SLAMF7, SH2D1A, TREML2, LILRA4
1269340	Hemostasis	1.10E–04	1.66E–03	1.08E–02	4.15E–02	22	SERPINA3, CD244, ITGAL, JAML, SIRPG, CD84, CFD, ADRA2A, RAC2, DOCK2, LCK, MMRN1, CD2, PIK3R6, P2RX5, TIMP1, JCHAIN, CD48, TMSB4X, PRKCB, IL2RB, IL2RG
1269543	Signaling by GPCR	2.62E–02	1.67E–01	1.00E+00	1.00E+00	28	GPR55, ADCYAP1R1, CCR2, SAA1, ADRA2A, PPP1R1B, XCL2, C3, CCR5, PLCB2, CCL13, CCL19, CCL21, CNR2, PNOC, RAC2, CXCR3, FGD2, WNT7A, WNT7B, RET, PIK3R6, WNT10A, PRKCB, ACKR1, IL2RB, IL2RG, S1PR4
Down-regulated genes							
1270189	Biological oxidations	3.08E–03	8.30E–02	5.43E–01	1.00E+00	9	CYP3A7, CYP2C8, CYP3A4, CYP4A11, CYP27B1, UGT2B7, CYP26B1, CYP4F2, GSTA2
1269544	GPCR ligand binding	1.59E–02	1.78E–01	1.00E + 00	1.00E+00	12	PYY, PTGER3, PTHLH, PLPPR4, CALCR, F2RL3, GPRC6A, CXCL2, CXCL3, UCN3, IHH, HCRTR2
1269903	Transmembrane transport of small molecules	3.20E–02	2.60E–01	1.00E + 00	1.00E+00	15	TRPM6, SLC26A4, SLC36A2, ATP6V1G3, ALB, ATP6V0D2, RHCG, ABCC11, SLC2A3, SLC4A1, SLC12A3, SLC26A7, SLC28A2, G6PC, GABRA2
1269203	Innate Immune System	2.61E–01	5.48E–01	1.00E+00	1.00E+00	20	NR4A1, CHI3L1, JUN, ATP6V1G3, BPI, FCN2, ATP6V0D2, MME, HSPA1B, FOS, DUSP1, DUSP2, APOB, MUC5B, MUC13, OLR1, SLC2A3, EGF, TREM1, CTSV
1269310	Cytokine signaling in immune system	5.39E–01	7.33E–01	1.00E+00	1.00E+00	10	JUNB, CCL3, FOS, DUSP1, DUSP2, CXCL2, OSM, EGF, EGR1, IL6
1268677	Metabolism of proteins	9.49E–01	9.74E–01	1.00E+00	1.00E+00	15	ADAMTS19, ADAMTS17, MME, KLK1, CALB1, ADAMTS4, NTNG1, MUC5B, XPNPEP2, MUC13, RGS7, IGF2, IGFBP1, ATF3

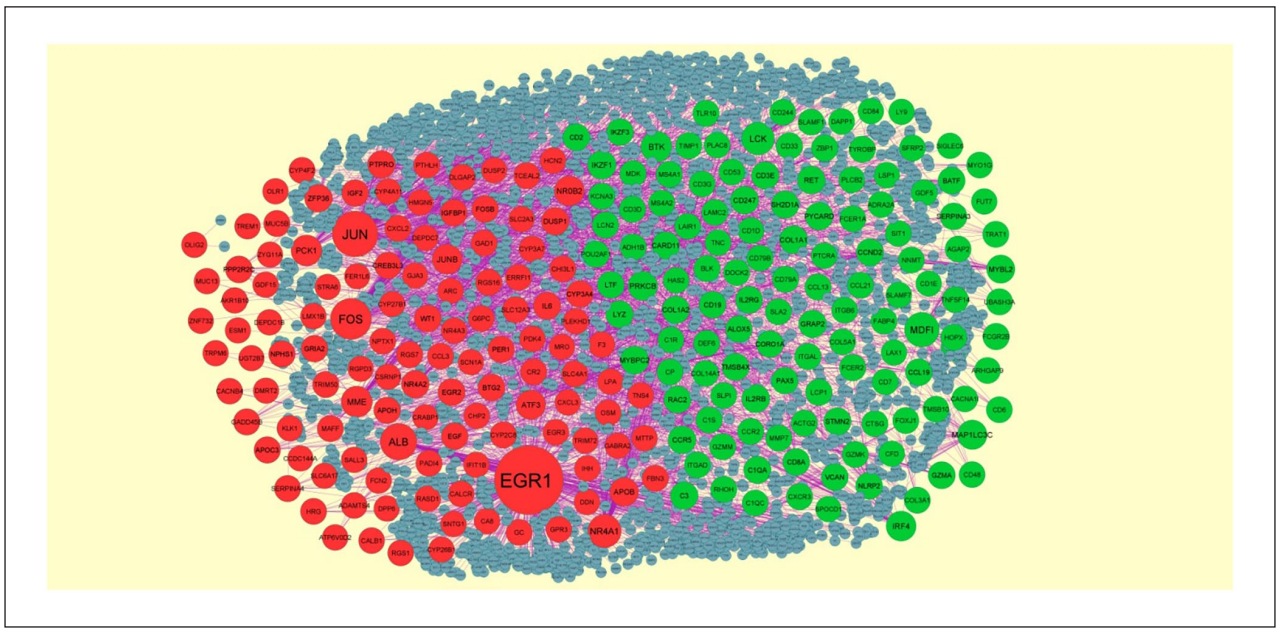

Figure 3. PPI network of DEGs. The PPI network of DEGs was constructed using Cytoscape. Upregulated genes are marked in green; down-regulated genes are marked in red.

specificity for the diagnosis of DN. As shown in Figure 7, MDFI, LCK, BTK, IRF4, PRKCB, EGR1, JUN, FOS, ALB, and NR4A1 achieved an AUC value of > 0.8, demonstrating that these hub genes have high sensitivity and specificity for DN diagnosis. The results suggested that MDFI, LCK, BTK, IRF4, PRKCB, EGR1, JUN, FOS, ALB, and NR4A1 can be used as biomarkers for the diagnosis of DN.

Discussion

DN affects millions of people all over the world.[30] DN occurs in uncontrolled diabetes, which is a worldwide complaint. The aim of this investigation was to screen and verify hub genes involved in DN as well as to explore potential molecular mechanisms.

In the present study, NGS data from GSE142025 were extracted to identify the DEGs between DN and normal control. In this investigation, we identified 549 DEGs, which includes 275 upregulated and 274 down-regulated genes. CFHR1[31] and RGS1[32] have been reported to altered expression in nephropathy. Studies have shown that GREM1 is linked with the progression of DN.[33] Existing evidence has reported that CCL19[34] is responsible for renal inflammation and fibrosis in DN. COL6A5[35] is associated with neuropathic chronic itch. Reports indicate that cell death-inducing DFFA-like effector c (CIDEC)[36] was found in the progression of obesity. NR4A1 drives DN growth through mitochondrial fission and mitophagy.[37] Recent study has reported that expression of NR4A2 is associated with myocardial infarction.[38] EGR1 is required for fibrosis and inflammatory response in DN.[39] ATF3 expression has been implicated in DN.[40] Altered expression of NR4A3 contributes to type 2 diabetes mellitus progression.[41] A previous study showed that the KLK1 gene is involved in DN.[42]

A series of DEGs was discovered to be enriched in the GO functions and pathways. Previous investigations have shown a signaling pathway that includes the innate immune system,[43] extracellular matrix organization,[44] hemostasis,[45] cytokine signaling in the immune system,[46] and metabolism of proteins,[47] which were associated with DN development. Previous studies had reported that expression of SERPINA3,[48] IKZF1,[49] BTK,[50] C1QA,[51] CD1C,[52] and CCL13[53] was correlated with lupus nephritis. Recent studies have demonstrated that the expression of TNFSF14,[54] ITGAL (integrin subunit alpha L),[55] PLAC8,[56] ADRA2A,[57] CCL21,[58] ALOX5,[59] CNR2,[60] COL1A1,[61] WNT7A,[62] SLAMF1,[63] CD3D,[64] lactotransferrin (LTF),[65] MIR27B,[66] PDK4,[67] UCN3,[68] PCK1,[69] carboxyl ester lipase (CEL),[70] TRPM6,[71] microsomal triglyceride transfer protein (MTTP),[72] CYP2 C8,[73] and CYP3A4[74] is associated with progression of type 2 diabetes mellitus. Recent studies have proposed that the altered expression of MZB1,[75] LAIR1,[76] MIR142,[77] and fibroblast activation protein alpha (FAP)[78] has been shown to be a meaningful advance factor for myocardial infarction. IRF4 plays a key role in obesity-induced insulin resistance.[79] Accumulating evidence showed that altered expression of genes such as midkine (MDK),[80] CCR2,[81] SAA1,[82] C3,[83] CD19,[84] CCR5,[85] CXCR3,[86] FABP4,[87] GDF15,[88] IGF2,[89] IGFBP1,[90] and IL6[91] is important in the progression of DN. A previous study has shown that UBASH3A,[92] signal regulatory protein gamma (SIRPG),[93] IKZF3,[94] CD1D,[95] CD2,[96] CD48,[97] CD247,[98] and CYP27B1[99] are liable for progression

Table 4. Topology table for up- and down-regulated genes.

Regulation	Node	Degree	Betweenness	Stress	Closeness
Up	MDFI	126	0.081127	4,626,488	0.320501
Up	LCK	98	0.049067	3,562,586	0.338404
Up	BTK	76	0.0377	38,70,178	0.332639
Up	IRF4	60	0.027138	2,609,572	0.323596
Up	PRKCB	53	0.026509	1,721,842	0.327185
Up	MAP1LC3C	53	0.031813	3,672,518	0.253337
Up	IKZF1	40	0.013119	1,148,684	0.316945
Up	COL1A1	36	0.015	1,185,640	0.317687
Up	MYBL2	36	0.015958	3,954,828	0.26938
Up	IL2RB	33	0.012158	1,042,652	0.355189
Up	RET	33	0.015085	724,266	0.347592
Up	MYBPC2	33	0.017333	1,527,886	0.265558
Up	CD247	32	0.008437	463,450	0.324758
Up	CCR5	31	0.014884	473,626	0.318919
Up	GRAP2	30	0.013154	639,080	0.322022
Up	C3	28	0.013842	992,764	0.301087
Up	CD3E	28	0.010192	547,816	0.321298
Up	PYCARD	28	0.01139	1,029,436	0.314084
Up	SH2D1A	27	0.011524	522,998	0.323018
Up	COL1A2	26	0.009445	611,534	0.347414
Up	RAC2	24	0.009511	633,510	0.295675
Up	STMN2	24	0.014359	649,404	0.307814
Up	CARD11	23	0.006165	483,588	0.313902
Up	CCND2	23	0.008353	708,408	0.312241
Up	LYZ	23	0.007853	530,116	0.313467
Up	TMSB4X	23	0.008343	714,442	0.311489
Up	C1QA	23	0.007755	632,982	0.265896
Up	GZMA	21	0.007666	963,298	0.270211
Up	IL2RG	20	0.006062	572,776	0.316797
Up	BATF	20	0.003837	254,330	0.296159
Up	IKZF3	19	0.005698	330,676	0.316538
Up	LTF	18	0.005184	456,248	0.314157
Up	VCAN	18	0.010548	416,498	0.310101
Up	NLRP2	18	0.006264	463,220	0.314229
Up	CD8A	18	0.006354	251,874	0.312098
Up	CD2	18	0.007228	336,022	0.319783
Up	CCL19	18	0.008406	553,768	0.308024
Up	SERPINA3	18	0.005921	300,382	0.28937
Up	CD19	17	0.003157	178,500	0.277903
Up	CORO1A	16	0.007864	466,092	0.307745
Up	PAX5	15	0.001643	214,276	0.280981
Up	ALOX5	15	0.006677	252,578	0.291389
Up	ITGAL	13	0.004138	316,950	0.296224
Up	CD33	13	0.002699	232,514	0.308339
Up	LCP1	13	0.003931	209,294	0.312133
Up	CD3D	13	0.003786	223,312	0.303071
Up	FCER2	13	0.001408	68,750	0.287378
Up	ADH1B	13	0.001997	278,048	0.267917
Up	FCGR2B	13	0.001497	99,768	0.275477
Up	ZBP1	13	0.006263	336,046	0.236205
Up	POU2AF1	13	0.00466	544,860	0.257666
Up	MDK	13	0.001715	115,114	0.241868
Up	TIMP1	12	0.004283	282,722	0.309288

(Continued)

Table 4. (Continued)

Regulation	Node	Degree	Betweenness	Stress	Closeness
Up	CD79A	12	0.003386	194,644	0.312889
Up	DOCK2	12	0.002561	173,086	0.309711
Up	TYROBP	12	0.005247	100,756	0.263905
Up	BLK	12	0.002074	70,518	0.308444
Up	GZMM	12	0.002889	174,370	0.255219
Up	LCN2	12	0.002886	523,816	0.277193
Up	UBASH3A	11	0.003708	227,440	0.307153
Up	KCNA3	11	0.004371	194,618	0.308199
Up	ACTG2	11	0.004953	290,190	0.310065
Up	CCR2	11	0.001733	114,362	0.265194
Up	CCL13	11	0.002461	173,840	0.273203
Up	CXCR3	11	0.002188	53,478	0.267626
Up	TLR10	11	0.004464	602,972	0.258279
Up	C1S	11	0.002249	144,728	0.275281
Up	RHOH	10	0.004278	206,936	0.305562
Up	FABP4	10	0.00375	501,850	0.235223
Up	MS4A1	10	0.002928	164,812	0.273534
Up	CTSG	10	0.002772	309,422	0.244725
Up	CD1D	10	0.001849	221,730	0.271835
Up	GZMK	10	0.003194	227,820	0.246817
Up	MMP7	10	0.003289	319,038	0.250785
Up	LAMC2	9	0.002248	178,286	0.294232
Up	GDF5	9	0.004743	147,730	0.297751
Up	MS4A2	9	0.001598	98,712	0.295482
Up	TRAT1	9	0.001536	65,702	0.283358
Up	TNFSF14	9	0.003776	324,884	0.250485
Up	COL3A1	9	0.001928	209,930	0.266758
Up	CP	8	0.00161	154,734	0.309853
Up	CD79B	8	0.001281	129,350	0.312637
Up	SLA2	8	0.001527	63,452	0.319031
Up	PLCB2	8	0.002326	133,780	0.291671
Up	CCL21	8	0.001558	34,922	0.25067
Up	HOPX	8	0.003087	329,986	0.266131
Up	FCER1A	8	9.12E–04	166,442	0.262832
Up	FOXJ1	8	0.004461	382,962	0.240198
Up	MYO1G	7	0.002723	207,766	0.293437
Up	NNMT	7	0.001827	170,236	0.311775
Up	ARHGAP9	7	0.001543	144,222	0.308865
Up	TMSB10	7	0.002711	168,816	0.307849
Up	COL5A1	7	0.002057	126,230	0.291702
Up	SLPI	7	0.001938	74,680	0.313504
Up	DEF6	7	0.001495	60,774	0.272135
Up	SLAMF1	7	0.001544	46,456	0.253337
Up	ITGAD	7	0.001325	131,106	0.256207
Up	ITGB6	7	0.001305	148,410	0.262806
Up	CD6	7	0.001789	182,212	0.235529
Up	CD3G	6	3.34E–04	82,462	0.297882
Up	COL14A1	6	0.001683	151,804	0.311274
Up	SIT1	6	3.89E–04	61,954	0.302328
Up	AGAP2	6	0.00305	177,840	0.294584
Up	TNC	6	9.89E–04	103,716	0.307884
Up	C1R	6	8.97E–04	61,888	0.286287
Up	CD48	6	0.001493	95,870	0.254573

(Continued)

Table 4. (Continued)

Regulation	Node	Degree	Betweenness	Stress	Closeness
Up	ADRA2A	6	0.002307	272,808	0.221587
Up	SFRP2	6	0.001594	133,652	0.242278
Up	LSP1	6	0.001784	49,576	0.262857
Up	CD244	6	1.15E–04	8570	0.258525
Up	C1QC	6	3.27E–04	30,566	0.242192
Up	CD53	6	0.001414	42,284	0.277704
Up	CD7	6	0.002235	142,468	0.229262
Up	TNNI2	6	0.002231	446,596	0.20216
Up	HAS2	5	8.86E–04	97,846	0.308129
Up	LAIR1	5	5.65E–04	89,664	0.309535
Up	PTCRA	5	0.001647	74,304	0.305081
Up	PLAC8	5	0.001118	152,116	0.309676
Up	CACNA1I	5	0.001737	61,034	0.260936
Up	DAPP1	5	0.00157	90,974	0.245589
Up	SLAMF7	2	4.70E–04	26,196	0.297751
Up	CFD	1	0	0	0.250762
Up	CD1E	1	0	0	0.290019
Up	SPOCD1	1	0	0	0.290019
Up	LAX1	1	0	0	0.243605
Up	FUT7	1	0	0	0.205279
Up	SIGLEC6	1	0	0	0.244175
Up	LY9	1	0	0	0.244175
Up	CD84	1	0	0	0.244175
Down	EGR1	518	0.346078	18,809,168	0.408427
Down	JUN	279	0.159961	12,725,726	0.39231
Down	FOS	214	0.100405	11,419,052	0.358995
Down	ALB	153	0.093571	6,530,500	0.334649
Down	NR4A1	107	0.060208	3,796,036	0.360234
Down	MME	78	0.048214	3,408,346	0.318171
Down	PCK1	74	0.042709	3,281,894	0.327067
Down	JUNB	62	0.016234	1,363,814	0.345205
Down	NR0B2	60	0.025162	3,689,286	0.320804
Down	ATF3	54	0.015604	1,820,748	0.339802
Down	APOB	43	0.021016	1,931,192	0.319219
Down	ZFP36	31	0.014411	625,526	0.345732
Down	DUSP1	30	0.009029	1,225,232	0.319069
Down	NR4A2	30	0.009805	2,286,296	0.267891
Down	PTPRO	29	0.014397	497,482	0.326045
Down	IL6	24	0.005225	1,052,826	0.278645
Down	EGR2	23	0.012011	387,098	0.34311
Down	WT1	21	0.011575	393,586	0.31106
Down	PPP2R2C	20	0.009443	506,060	0.30757
Down	BTG2	20	0.008629	576,654	0.307675
Down	CYP3A4	20	0.004079	665,634	0.284665
Down	IGFBP1	18	0.005608	765,806	0.272874
Down	IGF2	17	0.007236	235,938	0.265117
Down	FOSB	17	3.07E–04	41,372	0.292048
Down	EGF	17	0.004174	437,554	0.26858
Down	GRIA2	17	0.008456	649,690	0.233925
Down	CREB3L3	15	0.005393	659,206	0.251996
Down	APOH	15	0.004807	545,564	0.285955
Down	NPHS1	14	0.004565	192,324	0.31713
Down	APOC3	14	0.00416	339,034	0.306355

(Continued)

Table 4. (Continued)

Regulation	Node	Degree	Betweenness	Stress	Closeness
Down	PER1	14	0.005761	426,854	0.307745
Down	GADD45B	13	0.005219	293,026	0.34285
Down	FBN3	13	0.003392	454,688	0.249037
Down	CYP2C8	13	0.006838	502,454	0.266706
Down	RGS7	13	0.004132	270,892	0.279132
Down	RGS16	13	0.003611	353,032	0.265584
Down	TCEAL2	12	0.005928	617,496	0.300387
Down	SERPINA4	12	0.004309	117,754	0.288693
Down	SLC4A1	12	0.004598	370,504	0.260386
Down	MUC5B	11	0.003438	288,486	0.31131
Down	SLC12A3	11	0.003718	422,430	0.2988
Down	TRIM50	11	0.00539	372,840	0.296191
Down	MAFF	11	0.003754	525,420	0.259341
Down	CR2	11	0.003169	123,996	0.284159
Down	CCL3	11	0.003547	299,950	0.262476
Down	ERRFI1	11	0.001688	168,840	0.258206
Down	PADI4	11	0.003394	454,290	0.279938
Down	GC	11	0.002789	501,786	0.247763
Down	CXCL2	11	0.002319	457,378	0.253124
Down	CYP4F2	10	0.001747	352,720	0.314849
Down	DLGAP2	10	0.001402	167,204	0.260736
Down	PTHLH	10	0.002321	597,498	0.266392
Down	HRG	10	0.003161	259,838	0.256183
Down	CALCR	9	0.002726	106,854	0.24977
Down	GAD1	9	0.00311	125,432	0.292268
Down	CYP3A7	9	7.31E–04	191,768	0.261313
Down	NPTX1	8	0.003355	208,936	0.306805
Down	HCN2	8	0.002634	200,100	0.309605
Down	F3	8	0.003397	285,948	0.344242
Down	G6PC	8	0.001799	153,308	0.259837
Down	CHI3L1	8	4.74E–04	71,766	0.272517
Down	PDK4	7	0.002275	302,962	0.299261
Down	ADAMTS4	7	0.002892	176,694	0.296774
Down	OSM	7	0.002442	102,416	0.307501
Down	EGR3	7	4.62E–05	6350	0.304602
Down	CALB1	7	0.001944	134,650	0.263214
Down	CACNB4	6	0.002954	196,342	0.241309
Down	RASD1	6	9.38E–04	91,222	0.240646
Down	LMX1B	6	0.003032	239,712	0.245678
Down	NR4A3	6	0.001544	157,300	0.240987
Down	RGS1	6	0.001758	120,298	0.259465
Down	CHP2	5	0.001549	114,484	0.232105
Down	ATP6V0D2	5	0.002223	127,234	0.215277
Down	FCN2	5	1.19E–04	18,466	0.211124
Down	LPA	5	9.29E–04	39,398	0.266157
Down	SNTG1	4	0.001568	56,468	0.304602
Down	CA8	4	0.001168	70,098	0.29117
Down	TNS4	4	7.45E–04	60,554	0.305803
Down	SLC2A3	4	0.001604	126,392	0.293374
Down	GDF15	4	2.27E–04	48,866	0.300022
Down	SALL3	4	0.001568	56,468	0.304602
Down	MTTP	4	6.37E–05	5962	0.284308

(Continued)

Table 4. (Continued)

Regulation	Node	Degree	Betweenness	Stress	Closeness
Down	GPR3	4	0.00221	202,422	0.22101
Down	CXCL3	4	3.79E–04	68,926	0.267442
Down	OLR1	3	3.32E–04	58,030	0.292867
Down	DEPDC7	3	2.15E–04	16,336	0.291108
Down	GJA3	3	8.04E–04	39,932	0.291108
Down	MUC13	3	0.001474	66,414	0.291108
Down	DEPDC1B	3	0.001474	66,414	0.291108
Down	HMGN5	3	8.11E–04	78,088	0.292804
Down	TREM1	3	0.002489	38,934	0.292205
Down	AKR1B10	3	7.58E–04	52,706	0.224372
Down	CSRNP1	3	1.53E–04	18,490	0.224743
Down	CYP4A11	3	7.98E–05	17,838	0.208273
Down	TRIM72	3	8.13E–04	66,648	0.23153
Down	GABRA2	3	2.46E–04	30,422	0.239077
Down	DDN	3	7.42E–04	53,814	0.219526
Down	SCN1A	3	7.81E–04	41,474	0.19877
Down	TRPM6	3	0.001474	38,398	0.209107
Down	IHH	3	0.001474	99,214	0.194608
Down	CRABP1	3	0.001474	73,906	0.229883
Down	DUSP2	2	5.42E–05	35,462	0.307048
Down	ARC	2	7.37E–04	33,208	0.291046
Down	CYP26B1	2	4.18E–05	3986	0.222404
Down	KLK1	2	3.02E–05	1398	0.231887
Down	MRO	2	1.35E–05	4114	0.251227
Down	UGT2B7	2	7.37E–04	49,588	0.234147
Down	CYP27B1	2	9.02E–06	544	0.249059
Down	DPP6	2	1.75E–05	246	0.191181
Down	IFIT1B	2	7.37E–04	52,672	0.174019
Down	OLIG2	2	1	2	1
Down	DMRT2	1	0	0	0.290983
Down	CCDC144A	1	0	0	0.290983
Down	PLEKHD1	1	0	0	0.290983
Down	RGPD3	1	0	0	0.290983
Down	ZNF732	1	0	0	0.290983
Down	FER1L6	1	0	0	0.290983
Down	ZYG11A	1	0	0	0.290983
Down	STRA6	1	0	0	0.290983
Down	SLC6A17	1	0	0	0.290983
Down	ESM1	1	0	0	0.228547

of type 1 diabetes mellitus. The studies have shown that expression of SIT1,[100] junction adhesion molecule like (JAML),[101] TIMP1,[102] protein kinase C beta (PRKCB),[103] MMP7,[104] WNT7B,[105] WNT10A,[106] DUSP1,[107] WT1,[108] APOC3,[109] ERRFI1,[110] HCN2,[111] membrane metalloendopeptidase (MME),[112] STRA6,[113] SLC12A3,[114] and GC vitamin D-binding protein (GC)[115] expedites the epithelial-to-mesenchymal transition and renal fibrosis in DN. Previous studies have found complement factor D (CFD),[116] DOCK2,[117] lysozyme (LYZ),[118] CD5L,[119] SCARA5,[120] versican (VCAN),[121] GDF5,[122] SFRP2,[123] BTG2,[124] ZFP36,[125] GPR3,[126] OLR1,[127] PM20D1,[128] and UGT2B7[129] to be expressed in obesity. A study has confirmed that altered expression of FCRL3,[130] FCGR2B,[131] cartilage oligomeric matrix protein (COMP),[132] erythroferrone (ERFE),[133] and NPHS1[134] is involved in the progression of nephropathy. The expression of COL1A2,[135] LCK (LCK proto-oncogene, Src family tyrosine kinase),[136] LCN2,[137] and apolipoprotein B (APOB)[138] is key for the progression of diabetic retinopathy. Researchers showed that altered expression of COL3A1,[139] PER1,[140] JUN (Jun proto-oncogene, AP-1 transcription factor subunit),[141] SLC26A4,[142] F2RL3,[143] CYP4A11,[144] and CYP4F2[145] plays an important role in hypertension. Collectively, the results of enriched GO and

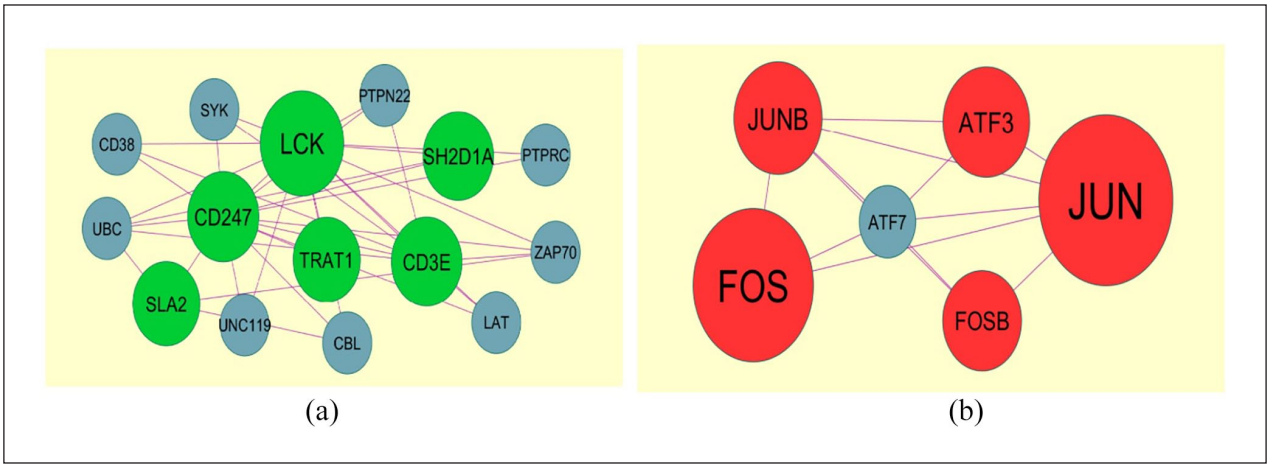

Figure 4. Significant modules of DEGs: (a) The most significant module was obtained from PPI network with 15 nodes and 36 edges for upregulated genes. (b) The most significant module was obtained from PPI network with seven nodes and 12 edges for upregulated genes. Upregulated genes are marked in green; down-regulated genes are marked in red.

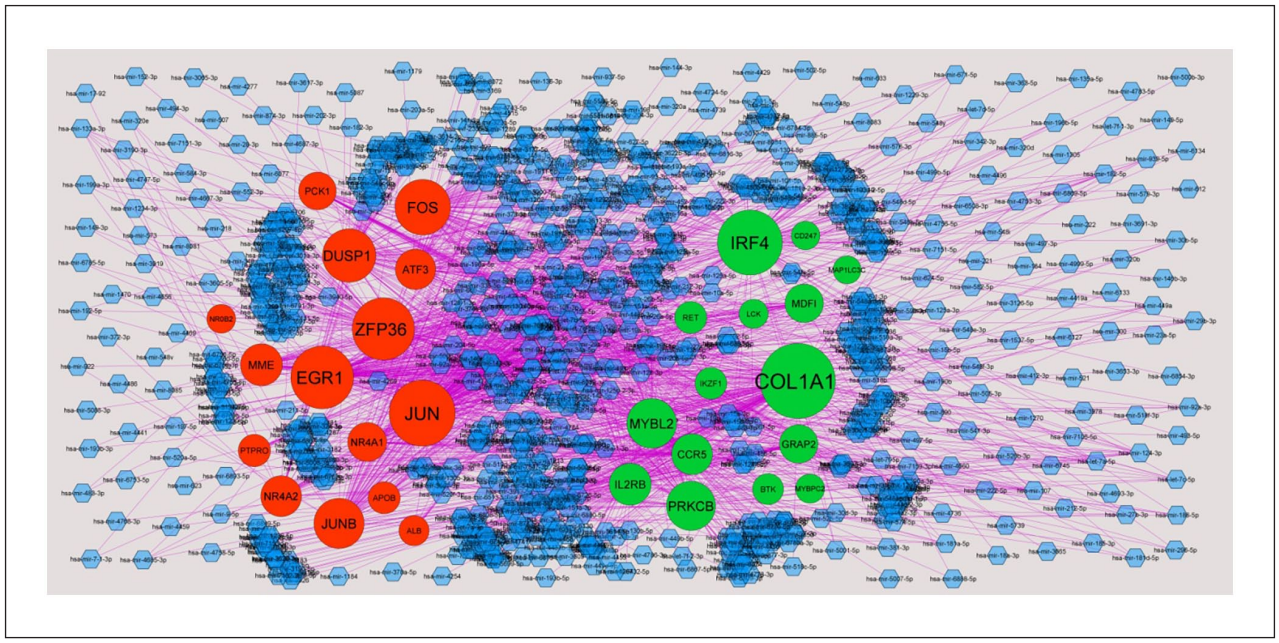

Figure 5. Target gene–miRNA regulatory network between target genes and miRNAs.
Upregulated genes are marked in green; down-regulated genes are marked in red. The blue color diamond nodes represent the key miRNAs.

REACTOME pathway enrichment analysis were positively correlated with experimental findings. However, further investigations are needed to explore and confirm the potentially significant pathways for DN and to achieve a comprehensive understanding of this process.

Based on the PPI network and module analysis, we obtained top hub genes in the whole network. Albumin (ALB)[146] has been shown as a promising biomarker in DN. In our study, correlations of MyoD family inhibitor (MDFI) and FOS (Fos proto-oncogene, AP-1 transcription factor subunit) with patient prognosis highlight the importance of these genes as novel biomarkers to stratify DN patients as well as potential therapeutic targets, but concrete roles of these genes need further investigation.

Based on the miRNA-DEG regulatory network and TF-DEG regulatory network, we obtained targets in the whole network. Recent recent investigation reported that the altered expression of MYBL2 was associated with myocardial infarction progression,[147] but this gene might be a novel target for DN. Many investigations have reported that expressions of hsa-mir-637[148] and NR3C1[149] were linked with the progression of hypertension, but these genes might be a novel target for DN. Hsa-mir-1261[150] has been shown to have an important role in DN. Hsa-mir-4458[151] has been

Table 5. miRNA–target gene and TF–target gene interaction.

Regulation	Target Genes	Degree	MicroRNA	Regulation	Target Genes	Degree	TF
Up	COL1A1	178	hsa-mir-4492	Up	IRF4	10	NFATC2
Up	IRF4	140	hsa-mir-4319	Up	LCK	10	YY1
Up	MYBL2	83	hsa-mir-637	Up	RET	10	NR2C2
Up	PRKCB	81	hsa-mir-1261	Up	MAP1LC3C	10	MAX
Up	IL2RB	54	hsa-mir-4300	Up	IL2RB	8	PDX1
Up	CCR5	50	hsa-mir-5193	Up	GRAP2	8	ELK1
Up	GRAP2	41	hsa-mir-3681-5p	Up	MYBPC2	7	RELA
Up	MDFI	41	hsa-mir-4441	Up	MDFI	6	TFAP2A
Up	RET	17	hsa-mir-129-2-3p	Up	MYBL2	6	GATA2
Up	IKZF1	16	hsa-mir-3607-3p	Up	CD247	5	SREBF1
Up	BTK	13	hsa-mir-4667-3p	Up	COL1A1	5	NFYA
Up	LCK	6	hsa-mir-210-3p	Up	PRKCB	4	IRF2
Up	MYBPC2	6	hsa-mir-214-3p	Up	IKZF1	4	E2F6
Up	CD247	4	hsa-mir-346	Up	BTK	2	SOX5
Up	MAP1LC3C	2	hsa-mir-27a-3p	Up	CCR5	1	EGR1
Down	JUN	144	hsa-mir-3943	Down	ATF3	19	TP53
Down	EGR1	132	hsa-mir-548e-3p	Down	EGR1	16	ARID3A
Down	ZFP36	130	hsa-mir-6077	Down	JUNB	15	SRF
Down	FOS	105	hsa-mir-5586-5p	Down	FOS	13	CREB1
Down	DUSP1	97	hsa-mir-4458	Down	PTPRO	12	NR3C1
Down	JUNB	85	hsa-mir-3065-5p	Down	NR0B2	11	USF1
Down	MME	54	hsa-mir-922	Down	MME	9	BRCA1
Down	NR4A2	50	hsa-mir-29b-2-5p	Down	JUN	9	SP1
Down	ATF3	48	hsa-mir-5000-5p	Down	DUSP1	9	STAT3
Down	NR4A1	43	hsa-mir-107	Down	NR4A1	9	HINFP
Down	PCK1	38	hsa-mir-1185-1-3p	Down	NR4A2	7	NR2E3
Down	PTPRO	18	hsa-mir-203a-3p	Down	PCK1	6	NR2F1
Down	APOB	17	hsa-mir-548p	Down	ZFP36	5	TFAP2C
Down	ALB	10	hsa-mir-492	Down	APOB	4	FOXA1
Down	NR0B2	5	hsa-mir-141-3p	Down	ALB	4	STAT1

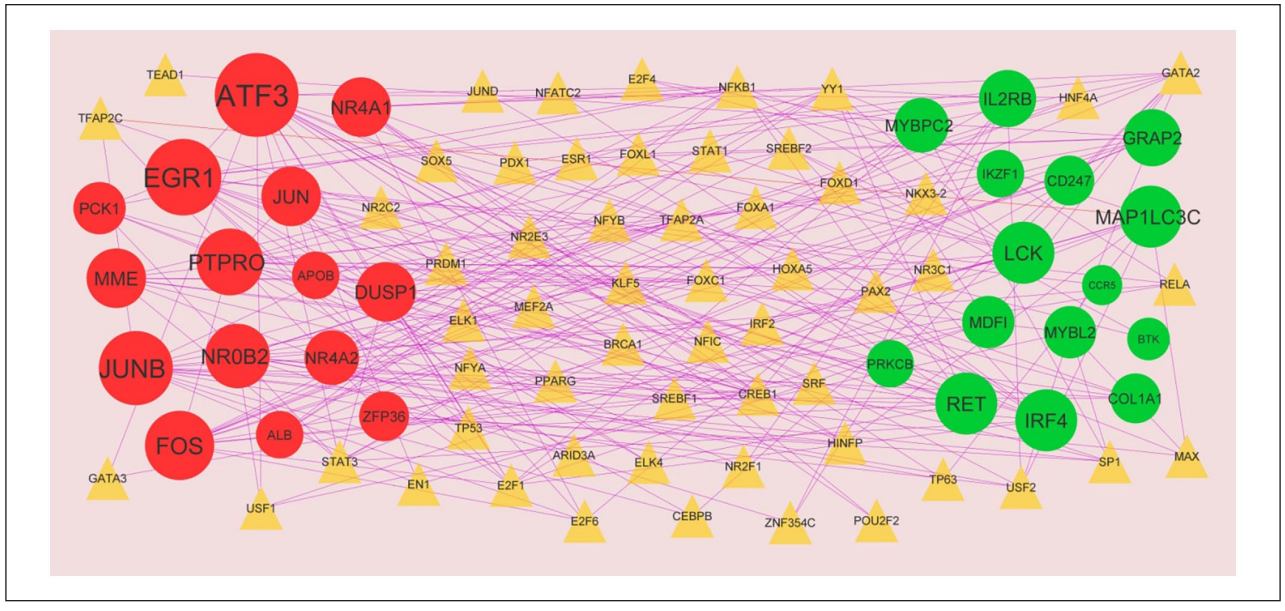

Figure 6. Target gene–TF regulatory network between target genes and TFs.
Upregulated genes are marked in green; down-regulated genes are marked in red. The blue color diamond nodes represent the key miRNAs. The yellow color triangle nodes represent the key TFs.

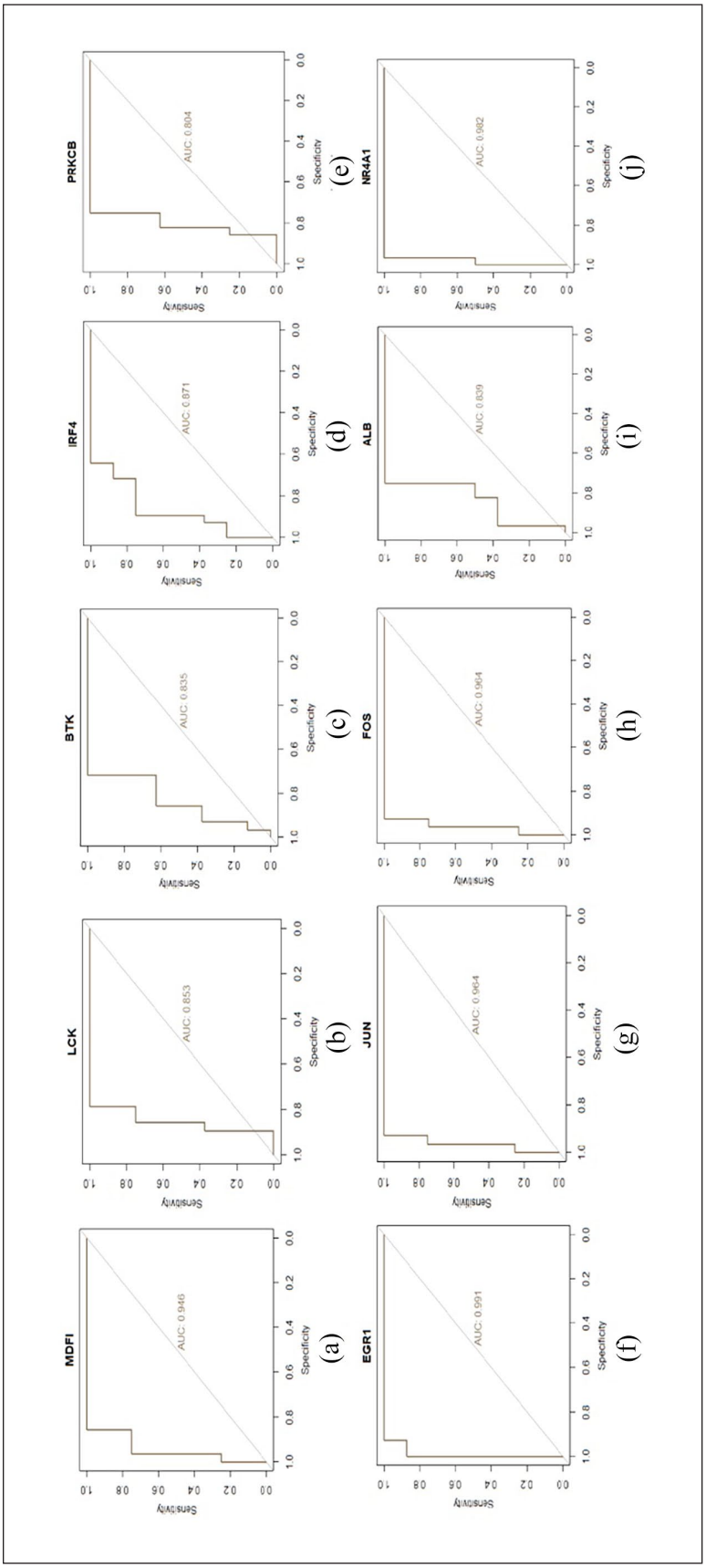

Figure 7. ROC curve validated the sensitivity, specificity of hub genes as a predictive biomarker for DN prognosis: (a) MDFI, (b) LCK, (c) BTK, (d) IRF4, (e) PRKCB, (f) EGR1, (g) JUN, (h) FOS, (i) ALB, and (j) NR4A1.

found to be differentially expressed in myocardial infarction, but this gene might be a novel target for DN. Recent studies have reported that expressions of NFATC2,[152] PDX1,[153] and CREB1[154] were involved in the progression of type 2 diabetes, but these genes might be a novel target for DN. Previous studies have demonstrated that expressions of YY1,[155] TP53[156] and serum-response factor (SRF)[157] played a key role in the progression of DN. IL2RB, hsa-mir-4492, hsa-mir-4319, hsa-mir-4300, hsa-mir-3943, hsa-mir-548e-3p, hsa-mir-6077, hsa-mir-5586-5p, RET (ret proto-oncogene), MAP1LC3C, PTPRO (protein tyrosine phosphatase receptor type O), NR2C2, myc-associated factor X (MAX), and ARID3A might be novel diagnostic biomarkers associated with the progression of DN, which remains to be verified based on a larger sample.

Besides, this investigation is purely a bioinformatics analysis without any in vivo and in vitro data. There are some limitations in our investigation. The lack of molecular and cellular evidence in wet-lab experiments imposes restrictions on the conclusions that can be drawn from our results.

Conclusion

In sum, based on a series of bioinformatics methods and a retrospective analysis, our identified 10 hub genes (MDFI, LCK, BTK, IRF4, PRKCB, EGR1, JUN, FOS, ALB, and NR4A1), which showed an intimate correlation with DN advancement and prognosis and had the potential acting as therapeutic targets and prognostic indicators. Further experiments are required to confirm the expression and potential functions of the identified key genes in DN.

Acknowledgements

The authors thank Weijia Zhang, Icahn School of Medicine at Mount Sinai, Renal, New York, USA, very much, the author who deposited their expression profiling by high-throughput sequencing data set, GSE142025, into the public GEO database. They also thank the preprint research square for providing information online; it is their pleasure to acknowledge their contributions.

Author contributions

H.J. contributed to Methodology and validation. B.V. contributed to Writing original draft, and review and editing. N.J. contributed to Software and resources. C.V. contributed to Investigation and resources.

Availability of data and materials

The data sets supporting the conclusions of this article are available in the GEO (Gene Expression Omnibus) (https://www.ncbi.nlm.nih.gov/geo/) repository. ((GSE142025) (https://www.ncbi.nlm.nih.gov/geo/query/acc.cgi?acc=GSE142025)

Declaration of conflicting interests

The author(s) declared no potential conflicts of interest with respect to the research, authorship, and/or publication of this article.

Ethical approval

This article does not contain any studies with human participants or animals performed by any of the authors.

Funding

The author(s) received no financial support for the research, authorship, and/or publication of this article.

Informed consent

No informed consent because this study does not contain human or animals participants.

ORCID iD

Chanabasayya Vastrad https://orcid.org/0000-0003-3615-4450

References

1. Papadopoulou-Marketou N, Chrousos GP and Kanaka-Gantenbein C. Diabetic nephropathy in type 1 diabetes: a review of early natural history, pathogenesis, and diagnosis. *Diabetes Metab Res Rev* 2017; 33(2): e2841.
2. Umanath K and Lewis JB. Update on diabetic nephropathy: core curriculum 2018. *Am J Kidney Dis* 2018; 71(6): 884–895.
3. Qi C, Mao X, Zhang Z, et al. Classification and differential diagnosis of diabetic nephropathy. *J Diabetes Res* 2017; 2017: 8637138.
4. Wang G, Ouyang J, Li S, et al. The analysis of risk factors for diabetic nephropathy progression and the construction of a prognostic database for chronic kidney diseases. *J Transl Med* 2019; 17(1): 264.
5. Heerspink HJ, Perkins BA, Fitchett DH, et al. Sodium glucose cotransporter 2 inhibitors in the treatment of diabetes mellitus: cardiovascular and kidney effects, potential mechanisms, and clinical applications. *Circulation* 2016; 134(10): 752–772.
6. Chen J, Luo SF, Yuan X, et al. Diabetic kidney disease-predisposing proinflammatory and profibrotic genes identified by weighted gene co-expression network analysis (WGCNA). *J Cell Biochem* 2022; 123(2): 481–492.
7. Lindholm E, Klannemark M, Agardh E, et al. Putative role of polymorphisms in UCP1-3 genes for diabetic nephropathy. *J Diabetes Complications* 2004; 18(2): 103–107.
8. Sun MY, Wang SJ, Li XQ, et al. CXCL6 promotes renal interstitial fibrosis in diabetic nephropathy by activating JAK/STAT3 signaling pathway. *Front Pharmacol* 2019; 10: 224.
9. Yang F, Cui Z, Deng H, et al. Identification of miRNAs-genes regulatory network in diabetic nephropathy based on bioinformatics analysis. *Medicine* 2019; 98(27): e16225.
10. Zeng M, Liu J, Yang W, et al. Identification of key biomarkers in diabetic nephropathy via bioinformatic analysis. *J Cell Biochem*. Epub ahead of print 2018. DOI: 10.1002/jcb.28155.
11. Zhang Y, Li W and Zhou Y. Identification of hub genes in diabetic kidney disease via multiple-microarray analysis. *Ann Transl Med* 2020; 8(16): 997.
12. Shang J, Wang S, Jiang Y, et al. Identification of key lncRNAs contributing to diabetic nephropathy by gene co-expression network analysis. *Sci Rep* 2019; 9(1): 3328.
13. Liao W, Jordaan G, Nham P, et al. Gene expression and splicing alterations analyzed by high throughput RNA sequencing of chronic lymphocytic leukemia specimens. *BMC Cancer* 2015; 15: 714.

14. Fan Y, Yi Z, D'Agati VD, et al. Erratum comparison of kidney transcriptomic profiles of early and advanced diabetic nephropathy reveals potential new mechanisms for disease progression. *Diabetes* 2020; 69(4): 797.
15. Clough E and Barrett T. The gene expression omnibus database. *Methods Mol Biol* 2016; 1418: 93–110.
16. Ferreira JA. The Benjamini-Hochberg method in the case of discrete test statistics. *Int J Biostat* 2007; 3(1): 11.
17. Chen J, Bardes EE, Aronow BJ, et al. ToppGene suite for gene list enrichment analysis and candidate gene prioritization. *Nucleic Acids Res* 2009; 37(Web Server Issue): w305–w 311.
18. Thomas PD. The gene ontology and the meaning of biological function. *Methods Mol Biol* 2017; 1446: 15–24.
19. Fabregat A, Jupe S, Matthews L, et al. Reactome pathway knowledgebase. *Nucleic Acids Res* 2018; 46(D1): D649–D655.
20. Breuer K, Foroushani AK, Laird MR, et al. InnateDB: systems biology of innate immunity and beyond—recent updates and continuing curation. *Nucleic Acids Res* 2013; 41(Database Issue): d1228–d1233.
21. Shannon P, Markiel A, Ozier O, et al. Cytoscape: a software environment for integrated models of biomolecular interaction networks. *Genome Res* 2003; 13(11): 2498–2504.
22. Przulj N, Wigle DA and Jurisica I. Functional topology in a network of protein interactions. *Bioinformatics* 2004; 20(3): 340–348.
23. Nguyen TP, Liu WC and Jordán F. Inferring pleiotropy by network analysis: linked diseases in the human PPI network. *BMC Syst Biol* 2011; 5: 179.
24. Shi Z and Zhang B. Fast network centrality analysis using GPUs. *BMC Bioinformatics* 2011; 12: 149.
25. Fadhal E, Gamieldien J and Mwambene EC. Protein interaction networks as metric spaces: a novel perspective on distribution of hubs. *BMC Syst Biol* 2014; 8: 6.
26. Zaki N, Efimov D and Berengueres J. Protein complex detection using interaction reliability assessment and weighted clustering coefficient. *BMC Bioinformatics* 2013; 14: 163.
27. Fan Y and Xia J. MiRNet-functional analysis and visual exploration of miRNA-target interactions in a network context. *Methods Mol Biol* 2018; 1819: 215–233.
28. Zhou G, Soufan O, Ewald J, et al. NetworkAnalyst 3.0: a visual analytics platform for comprehensive gene expression profiling and meta-analysis. *Nucleic Acids Res* 2019; 47: W234–W241.
29. Robin X, Turck N, Hainard A, et al. PROC: an open-source package for R and S+ to analyze and compare ROC curves. *BMC Bioinformatics* 2011; 12: 77.
30. Kishore L, Kaur N and Singh R. Distinct biomarkers for early diagnosis of diabetic nephropathy. *Curr Diabetes Rev* 2017; 13(6): 598–605.
31. Xie J, Kiryluk K, Li Y, et al. Fine mapping implicates a deletion of CFHR1 and CFHR3 in protection from IgA nephropathy in Han Chinese. *J Am Soc Nephrol* 2016; 27(10): 3187–3194.
32. Zhou XJ, Nath SK, Qi YY, et al. Novel identified associations of RGS1 and RASGRP1 variants in IgA nephropathy. *Sci Rep* 2016; 6: 35781.
33. McKnight AJ, Patterson CC, Pettigrew KA, et al. A GREM1 gene variant associates with diabetic nephropathy. *J Am Soc Nephrol* 2010; 21(5): 773–781.
34. Sun J, Wang J, Lu W, et al. MiR-325-3p inhibits renal inflammation and fibrosis by targeting CCL19 in diabetic nephropathy. *Clin Exp Pharmacol Physiol* 2020; 47(11): 1850–1860.
35. Martinelli-Boneschi F, Colombi M, Castori M, et al. COL6A5 variants in familial neuropathic chronic itch. *Brain* 2017; 140(3): 555–567.
36. Hall AM, Brunt EM, Klein S, et al. Hepatic expression of cell death-inducing DFFA-like effector C in obese subjects is reduced by marked weight loss. *Obesity* 2010; 18(2): 417–419.
37. Sheng J, Li H, Dai Q, et al. Promotes diabetic nephropathy by activating Mff-mediated mitochondrial fission and suppressing parkin-mediated mitophagy. *Cell Physiol Biochem* 2018; 48(4): 1675–1693.
38. Liu H, Liu P, Shi X, et al. NR4A2 protects cardiomyocytes against myocardial infarction injury by promoting autophagy. *Cell Death Discov* 2018; 4: 27.
39. Zha F, Qu X, Tang B, et al. Long non-coding RNA MEG3 promotes fibrosis and inflammatory response in diabetic nephropathy via miR-181a/Egr-1/TLR4 axis. *Aging* 2019; 11(11): 3716–3730.
40. Zhang H, Liang S, Du Y, et al. Inducible ATF3-NFAT axis aggravates podocyte injury. *J Mol Med* 2018; 96(1): 53–64.
41. Mohammad BS, Alireza N and Ramin S. The effect of NR4A3-rs12686676 and XBP1-rs2269577 polymorphisms on type 2 diabetes mellitus susceptibility in an Iranian population: case-control study. *Gene Reports* 21 2020; 20: 100854.
42. Riad A, Zhuo JL, Schultheiss HP, et al. The role of the renal kallikrein-kinin system in diabetic nephropathy. *Curr Opin Nephrol Hypertens* 2007; 16(1): 22–26.
43. Wada J and Makino H. Innate immunity in diabetes and diabetic nephropathy. *Nat Rev Nephrol* 2016; 12(1): 13–26.
44. Gerrits T, Zandbergen M, Wolterbeek R, et al. Endoglin promotes myofibroblast differentiation and extracellular matrix production in diabetic nephropathy. *Int J Mol Sci* 2020; 21(20): 7713.
45. Pan L, Ye Y, Wo M, et al. Clinical significance of hemostatic parameters in the prediction for type 2 diabetes mellitus and diabetic nephropathy. *Dis Markers* 2018; 2018: 5214376.
46. Liu Q, Xing L, Wang L, et al. Therapeutic effects of suppressors of cytokine signaling in diabetic nephropathy. *J Histochem Cytochem* 2014; 62(2): 119–128.
47. Tuttle KR. Linking metabolism and immunology: diabetic nephropathy is an inflammatory disease. *J Am Soc Nephrol* 2005; 16(6): 1537–1538.
48. Turnier JL, Brunner HI, Bennett M, et al. Discovery of SERPINA3 as a candidate urinary biomarker of lupus nephritis activity. *Rheumatology* 2019; 58(2): 321–330.
49. Zhang YM, Zhou XJ, Cheng FJ, et al. Association of the IKZF1 5' UTR variant rs1456896 with lupus nephritis in a northern Han Chinese population. *Scand J Rheumatol* 2017; 46(3): 210–214.
50. Kong W, Deng W, Sun Y, et al. Increased expression of Bruton's tyrosine kinase in peripheral blood is associated with lupus nephritis. *Clin Rheumatol* 2018; 37(1): 43–49.
51. Racila DM, Sontheimer CJ, Sheffield A, et al. Homozygous single nucleotide polymorphism of the complement C1QA gene is associated with decreased levels of C1q in patients

with subacute cutaneous lupus erythematosus. *Lupus* 2003; 12(2): 124–132.
52. Kassianos AJ, Wang X, Sampangi S, et al. Increased tubulointerstitial recruitment of human CD141(hi) CLEC9A(+) and CD1c(+) myeloid dendritic cell subsets in renal fibrosis and chronic kidney disease. *Am J Physiol Renal Physiol* 2013; 305(10): F1391–F1401.
53. Moreth K, Brodbeck R, Babelova A, et al. The proteoglycan biglycan regulates expression of the B cell chemoattractant CXCL13 and aggravates murine lupus nephritis. *J Clin Invest* 2010; 120(12): 4251–4272.
54. Halvorsen B, Santilli F, Scholz H, et al. LIGHT/TNFSF14 is increased in patients with type 2 diabetes mellitus and promotes islet cell dysfunction and endothelial cell inflammation in vitro. *Diabetologia* 2016; 59(10): 2134–2144.
55. Glawe JD, Patrick DR, Huang M, et al. Genetic deficiency of Itgb2 or ItgaL prevents autoimmune diabetes through distinctly different mechanisms in NOD/LtJ mice. *Diabetes* 2009; 58(6): 1292–1301.
56. Blue EK, Sheehan BM, Nuss ZV, et al. Epigenetic regulation of placenta-specific 8 contributes to altered function of endothelial colony-forming cells exposed to intrauterine gestational diabetes mellitus. *Diabetes* 2015; 64(7): 2664–2675.
57. Totomoch-Serra A, Muñoz ML, Burgueño J, et al. The ADRA2A rs553668 variant is associated with type 2 diabetes and five variants were associated at nominal significance levels in a population-based case-control study from Mexico City. *Gene* 2018; 669: 28–34.
58. Gonzalez Badillo FE, Zisi Tegou F, Abreu MM, et al. CCL21 expression in β-cells induces antigen-expressing stromal cell networks in the pancreas and prevents autoimmune diabetes in mice. *Diabetes* 2019; 68(10): 1990–2003.
59. Nejatian N, Häfner AK, Shoghi F, et al. 5-Lipoxygenase (ALOX5): Genetic susceptibility to type 2 diabetes and vitamin D effects on monocytes. *J Steroid Biochem Mol Biol* 2019; 187: 52–57.
60. de Luis DA, Izaola O, Primo D, et al. Polymorphism rs3123554 in the cannabinoid receptor gene type 2 (CNR2) reveals effects on body weight and insulin resistance in obese subjects. *Endocrinol Diabetes Nutr* 2017; 64(8): 440–445.
61. Tamagno G, Fedtke K, Eidenmüller M, et al. The polymorphism of type 1 collagen (COL1A1) gene does not correlate with an increased risk of foot ulcers in patients with diabetes mellitus. *Exp Clin Endocrinol Diabetes* 2015; 123(4): 240–245.
62. Wang W, Yan X, Lin Y, et al. Wnt7a promotes wound healing by regulation of angiogenesis and inflammation: issues on diabetes and obesity. *J Dermatol Sci* 2018; 91: 124–133.
63. Tabassum R, Mahajan A, Dwivedi OP, et al. Common variants of SLAMF1 and ITLN1 on 1q21 are associated with type 2 diabetes in Indian population. *J Hum Genet* 2012; 57(3): 184–190.
64. Aparicio JM, Wakisaka A, Takada A, et al. Non-HLA genetic factors and insulin dependent diabetes mellitus in the Japanese: TCRA, TCRB and TCRG, INS, THY1, CD3D and ETS1. *Dis Markers* 1990; 8(5): 283–294.
65. Mohamed WA and Schaalan MF. Antidiabetic efficacy of lactoferrin in type 2 diabetic pediatrics; controlling impact on PPAR-γ, SIRT-1, and TLR4 downstream signaling pathway. *Diabetol Metab Syndr* 2018; 10: 89.
66. Li H, Liu J, Wang Y, et al. MiR-27b augments bone marrow progenitor cell survival via suppressing the mitochondrial apoptotic pathway in type 2 diabetes. *Am J Physiol Endocrinol Metab* 2017; 313(4): E391–E401.
67. Kim YI, Lee FN, Choi WS, et al. Insulin regulation of skeletal muscle PDK4 mRNA expression is impaired in acute insulin-resistant states. *Diabetes* 2006; 55(8): 2311–2317.
68. Alarslan P, Unal Kocabas G, Demir I, et al. Increased urocortin 3 levels are associated with the risk of having type 2 diabetes mellitus. *J Diabetes* 2020; 12(6): 474–482.
69. Rees SD, Britten AC, Bellary S, et al. The promoter polymorphism -232C/G of the PCK1 gene is associated with type 2 diabetes in a UK-resident south Asian population. *BMC Med Genet* 2009; 10: 83.
70. Torsvik J, Johansson BB, Dalva M, et al. Endocytosis of secreted carboxyl ester lipase in a syndrome of diabetes and pancreatic exocrine dysfunction. *J Biol Chem* 2014; 289(42): 29097–29111.
71. Bouras H, Roig SR, Kurstjens S, et al. Metformin regulates TRPM6, a potential explanation for magnesium imbalance in type 2 diabetes patients. *Can J Physiol Pharmacol* 2020; 98(6): 400–411.
72. Lally S, Tan CY, Owens D, et al. Messenger RNA levels of genes involved in dysregulation of postprandial lipoproteins in type 2 diabetes: the role of Niemann-Pick C1-like 1, ATP-binding cassette, transporters G5 and G8, and of microsomal triglyceride transfer protein. *Diabetologia* 2006; 49(5): 1008–1016.
73. Dawed AY, Donnelly L, Tavendale R, et al. CYP2C8 and SLCO1B1 variants and therapeutic response to thiazolidinediones in patients with type 2 diabetes. *Diabetes Care* 2016; 39(11): 1902–1908.
74. Jamwal R, de la Monte SM, Ogasawara K, et al. Nonalcoholic fatty liver disease and diabetes are associated with decreased CYP3A4 protein expression and activity in human liver. *Mol Pharm* 2018; 15(7): 2621–2632.
75. Zhang L, Wang YN, Ju JM, et al. Mzb1 protects against myocardial infarction injury in mice via modulating mitochondrial function and alleviating inflammation. *Acta Pharmacol Sin* 2020; 42: 691–700.
76. Ellenbroek GHJM, de Haan JJ, van Klarenbosch BR, Brans MAD, et al. Leukocyte-associated immunoglobulin-like receptor-1 is regulated in human myocardial infarction but its absence does not affect infarct size in mice. *Sci Rep* 2017; 7(1): 18039.
77. Guo X, Chen Y, Lu Y, et al. High level of circulating microRNA-142 is associated with acute myocardial infarction and reduced survival. *Ir J Med Sci* 2020; 189(3): 933–937.
78. Tillmanns J, Hoffmann D, Habbaba Y, et al. Fibroblast activation protein alpha expression identifies activated fibroblasts after myocardial infarction. *J Mol Cell Cardiol* 2015; 87: 194–203.
79. Cavallari JF, Fullerton MD, Duggan BM, et al. Muramyl dipeptide-based postbiotics mitigate obesity-induced insulin resistance via IRF4. *Cell Metab* 2017; 25(5): 1063–1074.e3.
80. Kosugi T, Yuzawa Y, Sato W, et al. Midkine is involved in tubulointerstitial inflammation associated with diabetic nephropathy. *Lab Invest* 2007; 87(9): 903–913.
81. Gale JD, Gilbert S, Blumenthal S, et al. Effect of PF-04634817, an oral CCR2/5 chemokine receptor antagonist, on albuminuria

in adults with overt diabetic nephropathy. *Kidney Int Rep* 2018; 3(6): 1316–1327.
82. Kelly KJ, Zhang J, Han L, et al. Intravenous renal cell transplantation with SAA1-positive cells prevents the progression of chronic renal failure in rats with ischemic-diabetic nephropathy. *Am J Physiol Renal Physiol* 2013; 305(12): F1804–F1812.
83. Tang S, Wang X, Deng T, et al. Identification of C3 as a therapeutic target for diabetic nephropathy by bioinformatics analysis. *Sci Rep* 2020; 10(1): 13468.
84. Li T, Yu Z, Qu Z, et al. Decreased number of CD19+CD24hiCD38hi regulatory B cells in diabetic nephropathy. *Mol Immunol* 2019; 112: 233–239.
85. Yahya MJ, Ismail PB, Nordin NB, et al. Association of CCL2, CCR5, ELMO1, and IL8 polymorphism with diabetic nephropathy in Malaysian type 2 diabetic patients. *Int J Chronic Dis* 2019; 2019: 2053015.
86. Li MX, Zhao YF, Qiao HX, et al. CXCR3 knockdown protects against high glucose-induced podocyte apoptosis and inflammatory cytokine production at the onset of diabetic nephropathy. *Int J Clin Exp Pathol* 2017; 10(8): 8829–8838.
87. Ni X, Gu Y, Yu H, et al. Serum adipocyte fatty acid-binding protein 4 levels are independently associated with radioisotope glomerular filtration rate in type 2 diabetic patients with early diabetic nephropathy. *Biomed Res Int* 2018; 2018: 4578140.
88. Carlsson AC, Nowak C, Lind L, et al. Growth differentiation factor 15 (GDF-15) is a potential biomarker of both diabetic kidney disease and future cardiovascular events in cohorts of individuals with type 2 diabetes: a proteomics approach. *Ups J Med Sci* 2020; 125(1): 37–43.
89. Jing F, Zhao J, Jing X, et al. Long noncoding RNA Airn protects podocytes from diabetic nephropathy lesions via binding to Igf2bp2 and facilitating translation of Igf2 and lamb2. *Cell Biol Int* 2020; 44(9): 1860–1869.
90. Gu T, Falhammar H, Gu HF, et al. Epigenetic analyses of the insulin-like growth factor binding protein 1 gene in type 1 diabetes and diabetic nephropathy. *Clin Epigenetics* 2014; 6(1): 10.
91. Senthilkumar GP, Anithalekshmi MS, Yasir M, et al. Role of omentin 1 and IL-6 in type 2 diabetes mellitus patients with diabetic nephropathy. *Diabetes Metab Syndr* 2018; 12(1): 23–26.
92. Chen YG, Ciecko AE, Khaja S, et al. UBASH3A deficiency accelerates type 1 diabetes development and enhances salivary gland inflammation in NOD mice. *Sci Rep* 2020; 10(1): 12019.
93. Sinha S, Renavikar PS, Crawford MP, et al. Altered expression of SIRPγ on the T-cells of relapsing remitting multiple sclerosis and type 1 diabetes patients could potentiate effector responses from T-cells. *Plos One* 2020; 15(8): e0238070.
94. Burren OS, Guo H and Wallace C. VSEAMS: a pipeline for variant set enrichment analysis using summary GWAS data identifies IKZF3, BATF and ESRRA as key transcription factors in type 1 diabetes. *Bioinformatics* 2014; 30(23): 3342–3348.
95. Hussain S, Wagner M, Ly D, et al. Role of regulatory invariant CD1d-restricted natural killer T-cells in protection against type 1 diabetes. *Immunol Res* 2005; 31(3): 177–188.
96. Fraser HI, Howlett S, Clark J, et al. Ptpn22 and Cd2 variations are associated with altered protein expression and susceptibility to type 1 diabetes in nonobese diabetic mice. *J Immunol* 2015; 195(10): 4841–4852.
97. Ramos-Lopez E, Ghebru S, Van Autreve J, et al. Neither an intronic CA repeat within the CD48 gene nor the HERV-K18 polymorphisms are associated with type 1 diabetes. *Tissue Antigens* 2006; 68(2): 147–152.
98. Holmberg D, Ruikka K, Lindgren P, et al. Association of CD247 (CD3ζ) gene polymorphisms with T1D and AITD in the population of northern Sweden. *BMC Med Genet* 2016; 17(1): 70.
99. Hussein AG, Mohamed RH and Alghobashy AA. Synergism of CYP2R1 and CYP27B1 polymorphisms and susceptibility to type 1 diabetes in Egyptian children. *Cell Immunol* 2012; 279(1): 42–45.
100. Sun Z, Ma Y, Chen F, et al. MiR-133b and miR-199b knockdown attenuate TGF-β1-induced epithelial to mesenchymal transition and renal fibrosis by targeting SIRT1 in diabetic nephropathy. *Eur J Pharmacol* 2018; 837: 96–104.
101. Eftekhari A, Vahed SZ, Kavetskyy T, et al. Cell junction proteins: crossing the glomerular filtration barrier in diabetic nephropathy. *Int J Biol Macromol* 2020; 148: 475–482.
102. Wang J, Gao Y, Ma M, et al. Effect of miR-21 on renal fibrosis by regulating MMP-9 and TIMP1 in kk-ay diabetic nephropathy mice. *Cell Biochem Biophys* 2013; 67(2): 537–546.
103. Langham RG, Kelly DJ, Gow RM, et al. Increased renal gene transcription of protein kinase C-beta in human diabetic nephropathy: relationship to long-term glycaemic control. *Diabetologia* 2008; 51(4): 668–674.
104. Ban CR, Twigg SM, Franjic B, et al. Serum MMP-7 is increased in diabetic renal disease and diabetic diastolic dysfunction. *Diabetes Res Clin Pract* 2010; 87(3): 335–341.
105. McKay GJ, Kavanagh DH, Crean JK, et al. Bioinformatic evaluation of transcriptional regulation of WNT pathway genes with reference to diabetic nephropathy. *J Diabetes Res* 2016; 2016: 7684038.
106. Zhong JM, Lu YC and Zhang J. Dexmedetomidine reduces diabetic neuropathy pain in rats through the Wnt 10a/β-catenin signaling pathway. *Biomed Res Int* 2018; 2018: 904 3628.
107. Sheng J, Li H, Dai Q, et al. DUSP1 recuses diabetic nephropathy via repressing JNK-Mff-mitochondrial fission pathways. *J Cell Physiol* 2019; 234(3): 3043–3057.
108. Abe H, Sakurai A, Ono H, et al. Urinary exosomal mRNA of WT1 as diagnostic and prognostic biomarker for diabetic nephropathy. *J Med Invest* 2018; 65(34): 208–215.
109. Ng MC, Baum L, So WY, et al. Association of lipoprotein lipase S447X, apolipoprotein E exon 4, and apoC3 -455T>C polymorphisms on the susceptibility to diabetic nephropathy. *Clin Genet* 2006; 70(1): 20–28.
110. Asgarbeik S, Mohammad Amoli M, Enayati S, et al. The role of ERRFI1+808T/G polymorphism in diabetic nephropathy. *Int J Mol Cell Med* 2019; 8(Suppl. 1): 49–55.
111. Tsantoulas C, Laínez S, Wong S, et al. Hyperpolarization-activated cyclic nucleotide-gated 2 (HCN2) ion channels drive pain in mouse models of diabetic neuropathy. *Sci Transl Med* 2017; 9(409): eaam6072.

112. Zhang D, Gu T, Forsberg E, et al. Genetic and functional effects of membrane metalloendopeptidase on diabetic nephropathy development. *Am J Nephrol* 2011; 34(5): 483–490.
113. Chen CH, Lin KD, Ke LY, et al. O-GlcNAcylation disrupts STRA6-retinol signals in kidneys of diabetes. *Biochim Biophys Acta Gen Subj* 2019; 1863(6): 1059–1069.
114. De la Cruz-Cano E, Jiménez-González CDC, Morales-García V, et al. Arg913Gln variation of SLC12A3 gene is associated with diabetic nephropathy in type 2 diabetes and Gitelman syndrome: a systematic review. *BMC Nephrol* 2019; 20(1): 393.
115. Fawzy MS and Abu AlSel BT. Assessment of vitamin D-binding protein and early prediction of nephropathy in type 2 Saudi diabetic patients. *J Diabetes Res* 2018; 2018: 8517929.
116. Mathews JA, Wurmbrand AP, Ribeiro L, et al. Induction of IL-17A precedes development of airway hyperresponsiveness during diet-induced obesity and correlates with complement factor D. *Front Immunol* 2014; 5: 440.
117. Guo X, Li F, Xu Z, et al. DOCK2 deficiency mitigates HFD-induced obesity by reducing adipose tissue inflammation and increasing energy expenditure. *J Lipid Res* 2017; 58(9): 1777–1784.
118. Moreno-Navarrete JM, Latorre J, Lluch A, et al. Lysozyme is a component of the innate immune system linked to obesity associated-chronic low-grade inflammation and altered glucose tolerance. *Clin Nutr* 2020; 40: 1420–1429.
119. Wang L, Wang Y, Zhang C, et al. Inhibiting glycogen synthase kinase 3 reverses obesity-induced white adipose tissue inflammation by regulating apoptosis inhibitor of macrophage/CD5L-mediated macrophage migration. *Arterioscler Thromb Vasc Biol* 2018; 38(9): 2103–2116.
120. Lee H, Lee YJ, Choi H, et al. SCARA5 plays a critical role in the commitment of mesenchymal stem cells to adipogenesis. *Sci Rep* 2017; 7(1): 14833.
121. Han CY, Kang I, Harten IA, et al. Adipocyte-derived versican and macrophage-derived biglycan control adipose tissue inflammation in obesity. *Cell Rep* 2020; 31(13): 107818.
122. Zhang W, Wu X, Pei Z, et al. GDF5 promotes white adipose tissue thermogenesis via p38 MAPK signaling pathway. *DNA Cell Biol* 2019; 38(11): 1303–1312.
123. Crowley RK, O'Reilly MW, Bujalska IJ, et al. SFRP2 is associated with increased adiposity and VEGF expression. *PLoS ONE* 2016; 11(9): e0163777.
124. Gan M, Shen L, Wang S, et al. Genistein inhibits high fat diet-induced obesity through miR-222 by targeting BTG2 and adipor1. *Food Funct* 2020; 11(3): 2418–2426.
125. Caracciolo V, Young J, Gonzales D, et al. Myeloid-specific deletion of Zfp36 protects against insulin resistance and fatty liver in diet-induced obese mice. *Am J Physiol Endocrinol Metab* 2018; 315(4): E676–E693.
126. Godlewski G, Jourdan T, Szanda G, et al. Mice lacking GPR3 receptors display late-onset obese phenotype due to impaired thermogenic function in brown adipose tissue. *Sci Rep* 2015; 5: 14953.
127. Khaidakov M, Mitra S, Kang BY, et al. Oxidized LDL receptor 1 (OLR1) as a possible link between obesity, dyslipidemia and cancer. *PLoS ONE* 2011; 6(5): e20277.
128. Benson KK, Hu W, Weller AH, et al. Natural human genetic variation determines basal and inducible expression of PM20D1, an obesity-associated gene. *Proc Natl Acad Sci U S A* 2019; 116(46): 23232–23242.
129. Lloret-Linares C, Miyauchi E, Luo H, et al. Oral morphine pharmacokinetic in obesity: the role of P-glycoprotein, MRP2, MRP3, UGT2B7, and CYP3A4 jejunal contents and obesity-associated biomarkers. *Mol Pharm* 2016; 13(3): 766–773.
130. Zhang H, He Y, He X, et al. Three SNPs of FCRL3 and one SNP of MTMR3 are associated with immunoglobulin a nephropathy risk. *Immunobiology* 2020; 225(1): 151869.
131. Zhou XJ, Cheng FJ, Qi YY, et al. FCGR2B and FCRLB gene polymorphisms associated with IgA nephropathy. *PLoS ONE* 2013; 8(4): e61208.
132. Kosacka J, Nowicki M, Klöting N, et al. COMP-angiopoietin-1 recovers molecular biomarkers of neuropathy and improves vascularisation in sciatic nerve of ob/ob mice. *PLoS ONE* 2012; 7(3): e32881.
133. Hanudel MR, Rappaport M, Chua K, et al. Levels of the erythropoietin-responsive hormone erythroferrone in mice and humans with chronic kidney disease. *Haematologica* 2018; 103(4): e141–e142.
134. Bonomo JA, Ng MC, Palmer ND, et al. Coding variants in nephrin (NPHS1) and susceptibility to nephropathy in African Americans. *Clin J Am Soc Nephrol* 2014; 9(8): 1434–1440.
135. Zou J, Liu KC, Wang WP, et al. Circular RNA COL1A2 promotes angiogenesis via regulating miR-29b/VEGF axis in diabetic retinopathy. *Life Sci* 2020; 256: 117888.
136. Sergeys J, Van Hove I, Hu TT, et al. The retinal tyrosine kinome of diabetic Akimba mice highlights potential for specific Src family kinase inhibition in retinal vascular disease. *Exp Eye Res* 2020; 197: 108108.
137. Wang H, Lou H, Li Y, et al. Elevated vitreous Lipocalin-2 levels of patients with proliferative diabetic retinopathy. *BMC Ophthalmol* 2020; 20(1): 260.
138. Ankit BS, Mathur G, Agrawal RP, et al. Stronger relationship of serum apolipoprotein A-1 and B with diabetic retinopathy than traditional lipids. *Indian J Endocrinol Metab* 2017; 21(1): 102–105.
139. Samokhin AO, Stephens T, Wertheim BM, et al. NEDD9 targets COL3A1 to promote endothelial fibrosis and pulmonary arterial hypertension. *Sci Transl Med* 2018; 10(445): eaap7294.
140. Douma LG, Solocinski K, Holzworth MR, et al. Female C57BL/6J mice lacking the circadian clock protein PER1 are protected from nondipping hypertension. *Am J Physiol Regul Integr Comp Physiol* 2019; 316(1): R50–R58.
141. Altura BM, Kostellow AB, Zhang A, et al. Expression of the nuclear factor-kappaB and proto-oncogenes c-fos and c-jun are induced by low extracellular Mg2+ in aortic and cerebral vascular smooth muscle cells: possible links to hypertension, atherogenesis, and stroke. *Am J Hypertens* 2003; 16(9 Pt. 1): 701–707.
142. Kim BG, Yoo TH, Yoo JE, et al. Resistance to hypertension and high Cl- excretion in humans with SLC26A4 mutations. *Clin Genet* 2017; 91(3): 448–452.
143. Gao BF, Shen ZC, Bian WS, et al. Correlation of hypertension and F2RL3 gene methylation with prognosis of coronary heart disease. *J Biol Regul Homeost Agents* 2018; 32(6): 1539–1544.

144. Williams JS, Hopkins PN, Jeunemaitre X, et al. CYP4A11 T8590C polymorphism, salt-sensitive hypertension, and renal blood flow. *J Hypertens* 2011; 29(10): 1913–1918.
145. Geng H, Li B, Wang Y, et al. Association between the CYP4F2 gene rs1558139 and rs2108622 polymorphisms and hypertension: a meta-analysis. *Genet Test Mol Biomarkers* 2019; 23(5): 342–347.
146. Onions KL, Gamez M, Buckner NR, et al. VEGFC reduces glomerular albumin permeability and protects against alterations in VEGF receptor expression in diabetic nephropathy. *Diabetes* 2019; 68(1): 172–187.
147. Rafatian G, Kamkar M, Parent S, et al. Mybl2 rejuvenates heart explant-derived cells from aged donors after myocardial infarction. *Aging Cell* 2020; 19(7): e13174.
148. Cengiz M, Karatas OF, Koparir E, et al. Differential expression of hypertension-associated microRNAs in the plasma of patients with white coat hypertension. *Medicine* 2015; 94(13): e693.
149. Hogewind BF, Micheal S, Schoenmaker-Koller FE, et al. Analyses of sequence variants in the MYOC gene and of single nucleotide polymorphisms in the NR3C1 and FKBP5 genes in corticosteroid-induced ocular hypertension. *Ophthalmic Genet* 2015; 36(4): 299–302.
150. Wang J, Wang G, Liang Y, et al. Expression profiling and clinical significance of plasma microRNAs in diabetic nephropathy. *J Diabetes Res* 2019; 2019: 5204394.
151. Li Y, He XN, Li C, et al. Identification of candidate genes and microRNAs for acute myocardial infarction by weighted gene coexpression network analysis. *Biomed Res Int* 2019; 2019: 5742608.
152. Keller MP, Paul PK, Rabaglia ME, et al. The transcription factor Nfatc2 regulates β-cell proliferation and genes associated with type 2 diabetes in mouse and human islets. *PLoS Genet* 2016; 12(12): e1006466.
153. Fujimoto K, Chen Y, Polonsky KS, et al. Targeting cyclophilin D and the mitochondrial permeability transition enhances beta-cell survival and prevents diabetes in Pdx1 deficiency. *Proc Natl Acad Sci U S A* 2010; 107(22): 10214–10219.
154. Xu Y, Song R, Long W, et al. CREB1 functional polymorphisms modulating promoter transcriptional activity are associated with type 2 diabetes mellitus risk in Chinese population. *Gene* 2018; 665: 133–140.
155. Du L, Qian X, Li Y, et al. Sirt1 inhibits renal tubular cell epithelial-mesenchymal transition through YY1 deacetylation in diabetic nephropathy. *Acta Pharmacol Sin* 2020; 42: 242–251.
156. Zhang SZ, Qiu XJ, Dong SS, et al. MicroRNA-770-5p is involved in the development of diabetic nephropathy through regulating podocyte apoptosis by targeting TP53 regulated inhibitor of apoptosis 1. *Eur Rev Med Pharmacol Sci* 2019; 23(3): 1248–1256.
157. Zhao L, Chi L, Zhao J, et al. Serum response factor provokes epithelial-mesenchymal transition in renal tubular epithelial cells of diabetic nephropathy. *Physiol Genomics* 2016; 48(8): 580–588.